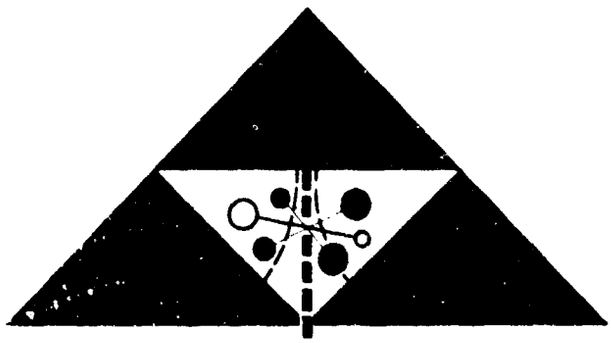

ARD-253

SUMMARY REPORT - INVESTIGATION OF A RESONANT COMBUSTOR CONCEPT

PHASE II of Contract No. Nonr 2458(00)
supported by the Power Branch of the
Office of Naval Research

Report No. ARD-253

30 January 1960

SUMMARY REPORT - INVESTIGATION OF A RESONANT COMBUSTOR CONCEPT

PHASE II of Contract No. Nonr 2458(00) Supported by the Power Branch of the Office of Naval Research

George E. Heuer, Senior Engineer
Raymond M. Lockwood, Principal Investigator

Propulsion Department

ADVANCED RESEARCH
DIVISION OF HILLER AIRCRAFT CORPORATION

SYMBOLS

A	cross sectional area
F_n	net thrust gain due to combustion
P	pressure
q	velocity head
T	temperature
W_A	air weight flow rate
W_f	fuel weight flow rate
W_4	$W_A + W_f$
δ	$\frac{P_o}{P_{osl}}$, where $P_{osl} = 29.92"$ Hg
θ	$\frac{T_{2T}}{T_{osl}}$, where $T_{osl} = 520^oR$
η_B	combustion efficiency

Subscripts

T	Total
sl	Sea level standard conditions
1, 2, 3, 4	as indicated in sketch, Figure (23)

LIST OF FIGURES

TABLE OF CONTENTS

1. SUMMARY

This project is concerned with an attempt to take advantage of the pressure rise that occurs during resonant combustion, but to avoid the losses that have plagued the majority of resonant combustion systems during the blowback or flow reversal portion of the cycle. In order to avoid flow reversal losses as well as to take advantage of a ram pressure rise (or compressor pressure rise), the resonant combustor was placed inside a ram shroud or duct which permits a bypass flow around the combustor. A large number of combustor air inlets were provided (between 80 and 100 inlets), which permitted submerging the inlets into the combustor shell, and thus reducing the external drag around the combustor and improving the combustor air inflow coefficient.

The use of a large number of air inlets also contributed to a reduction of burning time, which was reflected in an unusually high operating frequency. Fuel was injected into each air inlet in a jet pump arrangement. This feature permitted static (zero airspeed) starting and operation of the combustor when using gaseous fuels such as propane.

The air inlets were initially arranged perpendicular to the combustor shell, i.e., perpendicular to the longitudinal axis of the combustor, but a new combustor was developed during 1959 and evaluated in connected-pipe tests. It has the flush air inlets slanted at 45° to the combustor axis so that the blowback is directed aft. This slanting of the air inlets has resulted in a pressure-gain combustion system with higher performance than the configuration with orthogonal inlets.

Starting with static operation, the combustion was shown to be

quite complete as exhaust gas samples typically showed less than one percent combustibles.

The configuration investigated was marked by a contrasting combination of high combustion efficiency, and a mild pressure-gain mode of combustion, but with a relatively poor thrust specific fuel consumption. It is believed that the latter was partly due to poor matching between the shroud nozzle arrangement and the combustor. Tests revealed a trend of improved thrust specific fuel consumption with increase of simulated airspeed. The variation of shroud overhang length shows that there is an optimum length of shroud overhang beyond the end of the combustor, which infers that there is a tuning effect between the natural frequency of the combustor and the surrounding shroud. The results of the investigation support the contention that resonant, valveless combustor configurations can be devised to be operationally compatible with ram shrouds which enclose them and operate over a wide range of fuel flow rates. Best overall shrouded resonant combustor performance over the entire range from zero airspeed to high subsonic airspeed, can be expected from a combustor with highest static (i.e., zero air speed) combustion chamber pressure (or specific thrust) and lowest static thrust specific fuel consumption. This statement is dependent upon the requirement that the configurations must be arranged so that combustion exhaust gases do not interfere with the inflow into the ram-shroud but rather are by-passed around the combustor within the shroud during the pressure-rise portion of the combustion cycle.

It is recommended that a succeeding phase of work be based on the investigation of paired U-tube combustors operating 180° out-of-phase within a common ram shroud.

2. INTRODUCTION

2.1 Basic Concepts

The main purpose of this Phase II study, and of the previously completed Phase I study, has been to develop a combustor for high air speed operation that takes advantage of the qualities of resonant combustion.

As explained in Reference (2), "Resonant Combustion can combine high combustion efficiency with a pressure rise during combustion. By contrast, in steady flow combustion, in which some pressure loss always occurs, it is characteristic that maximum combustion efficiency and minimum pressure loss in the same burner configuration are incompatible. In other words, combustion efficiency in the steady flow case is gained at the expense of increasing the combustion pressure loss or vice-versa. The advantages of resonant combustion are rather widely known. However, as air speed increases, air inflow losses have been shown to increase at a higher rate than is typical of steady flow air breathing jet engines. This characteristic performance reduction with increasing air speed has been the most critical factor in preventing more widespread use of engines using resonant or intermittent combustion. There is some reason to believe that the concepts employed in the Phase I and Phase II studies may improve the utilization of resonant combustion in high speed valveless pulsejets, and may also make it practicable to use this type of combustion in gas turbine cycles."

As indicated in Reference (1), and illustrated in Figures (1), (3), and (4), the basic concepts involved in this resonant combustor research

are as follows: (1) fuel is introduced through a multitude of injector (jet pump) inlets; (2) air inflow is initially induced and is continued by the jet pumping action of the fuel nozzles, and a significant amount of mixing of fuel and air occurs in the inlet; (3) the inner ends of the air inlet tubes, when heated, act as multiple sources of ignition; (4) this method of induction of fuel and air through multiple jet pump inlets should cause violent mixing and stirring in the combustor. The net result of these concepts is to increase the effective burning rate, that is, decrease the combustion cycle time, which, generally speaking, contributes towards improved cycle efficiency.

In Phases I and II of the study, the combustor was shrouded as shown in Figure (2), to reduce the losses associated with air inflow to the combustion chamber. The advantages are apparent. The duct around the resonant burner enables the designer to utilize the pressure rise available from ram air, through the use of a good diffuser on the duct inlet. It is not practicable to apply a high-speed diffuser directly to a pulsejet air inlet because of the high losses that occur during the reverse flow or blow-back portion of the operating cycle, when the combustion pressure rises above the inlet pressure. The placing of a duct around the resonant burner permits the burner to operate in an environment in which the kinetic energy of the air is lower than that in the surrounding free air stream. In this situation, when combustion pressure suddenly rises above the inlet pressure, the blow-back is directed into the shroud. The pressure loss is not now so great because (1) the inlet air has first been slowed down in the shroud diffuser and (2) the majority of the blow-back is discharged

into the shroud that surrounds the burner. This blow-back does prevent inflow to the burner, but the shroud air can bypass the burner during this portion of the engine cycle, which has the effect of reducing shock loss at the shroud diffuser. Furthermore, transverse or slanted discharge of the blow-back gases into the shroud bypass airstream is believed to cause less disturbance in the diffuser than if the blow-back were pointed directly upstream into the shroud diffuser. Phase I work dealt with inlets oriented transversely to the shroud airstream. Phase II work studied the effects of angling the inlets in several directions, including "downstream" so that the blow-back was directed partly in the downstream direction.

2.2 Phase I Development

As a direct result of the Phase I study, the combustor configuration, inlet area, and arrangement of inlets necessary to support resonant combustion were predictable for the Phase II test hardware. The work done and progress achieved in Phase I is briefly described in the Summary of Reference (2), and is quoted verbatim below.

> "A new resonant combustor concept has proceeded to the point of initial evaluation. A shrouded resonant combustor with multiple ejector-type air inlets has been constructed and demonstrated. The main purpose of this research has been to achieve a combustor that can take advantage of the qualities of resonant combustion (a combination of high combustion efficiency with a pressure rise during combustion) without suffering from the air inflow losses

characteristic of resonant combustion with increasing airspeed."

"The cycle frequency of this resonant combustor is indicative of a very low burning time (high burning rate) which was expected to be a feature of the concept due to introduction of fuel and air through a very large number of inlets. The ducted concept permits air to bypass the basic combustor, which is an important feature in reducing losses due to blow-back through the air inlets during combustion. The shroud diffuser provides a ram pressure rise."

"The combustor was evolved in unducted static development testing from a burner with seven cylindrical inlets that protruded from the combustor shell, to a burner with as many as one hundred fuel and air inlets that are flush with the outer surface of the shell. Hardware was designed to permit rapid variation of combustor parameters that affected resonant operation in the static unducted environment."

"The connected-pipe test results presented were taken with a burner that was evolved in unducted static development testing. The only significant variation of parameters undertaken during connected-pipe testing was a variation of duct overhang and some increase of fuel jet orifice size. Furthermore, only one intermediate fuel flow rate was taken for each air flow rate, rather than a range of fuel flow rates from lean-out to rich-out."

"More detailed testing and optimization of parameters for ducted operation is planned for Phase II."

2.3 Phase II Objectives

The objectives of the Phase II Resonant Combustion program were to determine the following characteristics of the shrouded burner:

a) combustion efficiency

b) total pressure loss or gain across burner

c) heat release rate (BTU/hr/cu.ft.)

d) starting characteristics

e) combustor pulsation frequency and amplitude

f) effect of acoustical attenuation and resonant characteristics of inlet and exhaust attachments that approximate gas turbine and ramjet applications

In addition, transition to liquid fuel injection would be made.

2.4 Developmental Approach

2.4.1 Static Burner Testing and Development

As in the Phase I program, static burner testing and development was first conducted to eliminate some variables and to discover trends which would be useful in the construction and testing of a shrouded multiple-inlet burner for use in connected-pipe tests.

2.4.2 Connected-Pipe Burner Testing and Development

Based on the results and conclusions of the static burner testing, as reported in Reference (4), a multiple-inlet shrouded burner was constructed.

This burner incorporated a large number (80) of small inlets, with inlet orientation and physical characteristics based on the conclusions of the static burner testing (see Figures 9 and 10). This shrouded burner was connected to a "ram" air supply and tests were conducted to determine system variables and trends and the effects of configuration changes on these trends.

3. EXPERIMENTAL PROCEDURE AND RESULTS

3.1 Static Tests and Results

A full report of the static tests conducted, and the results thereof, is presented in Reference (4), which constituted Progress Report No. 3 of this phase of this contract. The static testing showed the effects of varying combustor elements, and indicated trends and conclusions which are enumerated below. The specific effects studied were (see Figure 8):

a) direction of inlet inclination

b) fuel nozzle penetration into inlet

c) inlet tube penetration into combustion chamber

d) inlet tube length

In addition, a general observation of the effects of combustor length and exhaust configuration was conducted.

3.1.1 Inlet Configurations

Inlet tubes were inclined 45° upstream, 45° downstream, at 90° to the burner axis, and at 90° to the burner axis but tangential to the burner (see Figure 8). Evaluation of each configuration was based on thrust produced, burner head pressure, combustor length, resonant starting ability, and range of fuel flow rates over which resonant combustion would occur. It was recognized that burner head pressure might be a misleading criterion, since a rise or reduction in burner head pressure with a particular configuration might indicate a change in position of pressure concentration within the combustor, rather than a rise or reduction in overall combustor pressure.

The superiority of the 45° downstream-angled inlets is shown in

Figures (12) and (13). Relative to the 45° downstream inlet configuration, the performance of the other inlet configurations was found to be less desirable in the following respects:

3.1.1. 90° Tangential Inlet

The 90° tangential inlet configuration produced thrust vs fuel flow about equal to the 45° downstream inlets, but with a very much lower burner head pressure and over a smaller range of fuel flows. Further, the burner length necessary to achieve this was almost double the optimum length for 45° downstream inlets.

3.1.1.2 45° Upstream Inlet

With inlets inclined 45° upstream, thrust and burner head pressure were appreciably reduced, and the range of resonating fuel flow rates was lower.

3.1.1.3 90° Inlet

The 90° inlets, although providing generally equivalent thrust to the 45° downstream inlets, gave a lower burner head pressure and a lower resonating fuel flow range. Further, the 90° inlets resulted in a significant falling off of thrust at the top of the fuel flow range.

3.1.2 Burner Length and Exhaust Diameter, 45° Downstream Inlets

The 45° downstream inlet configuration, being judged the superior configuration of the several tested, was used in additional tests to determine the effects of burner length and exhaust diameter. Burner length was varied from 25-3/8" to 45-5/8", within which range three exhaust diameters were tested on the four inch diameter combuster (see Figure 8):

a) 4" diameter (unaltered)

b) 3-1/2" diameter (nozzle affixed)

c) 5" diameter (diffuser affixed)

The best configuration appeared to be 30-5/8" burner length with exhaust diffused to 5" diameter.

3.1.3 Fuel Nozzle Penetration into Inlet

Using the 45° downstream inlet configuration with 30-5/8" burner length and exhaust diffusion to 5" diameter, the effect of depth of fuel nozzle penetration into the inlet tube was investigated. The effect is quite pronounced. Four positions were investigated:

1) nozzle 1/4" outside plane of inlet tube entrance

2) nozzle in plane of inlet tube entrance

3) nozzle projecting 1/4" into inlet tube

4) nozzle projecting 1/2" into inlet tube

The position with nozzles in the plane of the inlet tube entrance gave the best results, resulting in thrust and burner head pressure higher than with nozzles 1/4" outside the inlet tube entrance plane. With nozzles projecting into the inlet tubes 1/4" and 1/2", resonant burning would not commence without an air blast.

3.1.4 Inlet Tube Penetration into Combustion Chamber

The effect of distance of inlet tube penetration into the combustion chamber was investigated, with the 45° downstream inlets, 30-5/8" burner length, and exhaust diffusion to 5" diameter. From Figure (6), sketch (a), it is seen that the inlet tubes were mounted in inlet bushings. The distance

of penetration into the combustion chamber could then be varied by moving the inlet tubes axially. Tests were made with the inlet tubes flush with the inner ends of the bushings, with the inlet tubes extending 1/4", 1/2" and 3/4" beyond the ends of the bushings, and with the inlet tubes scarfed 45° on the ends to make the plane of the inlet end parallel to the longitudinal axis of the burner. In general, the highest thrust was obtained with the inlets flush with the bushing ends or protruding 1/4", and the lowest with the scarfed inlet ends. Resonant burning was possible at all positions.

3.1.5 Inlet Tube Length

Starting with an inlet tube length of 3", the tubes were reduced to 2-3/8" length, then scarfed 45° on the inner ends, and finally reduced to 1-11/16" length. Performance deteriorated noticeably as the inlet tube length was reduced, although resonance and the resonating fuel flow range did not appear to be affected until the tube length was reduced to 1-11/16" ($\frac{L}{D} = 3.0$).

3.1.6 Conclusions Derived from Static Testing

The static burner testing led to a number of conclusions, which were reported in Reference (4) and which are repeated here, as follows:

(1) "For any given burner configuration, thrust varies approximately linearly with average pressure across the burner head over most of the fuel flow range, but not necessarily with fuel flow rate. Near rich-out, the thrust begins to lag, and may even reverse with some configurations.

(2) "For a particular burner, each direction of inlet tube into the combustion chamber provides a characteristic of thrust vs average burner head pressure peculiar to that direction of inlets, and the effect of inlet direction on burner performance is very strong.

(3) "For a given burner configuration, lengthening of the burner results in easier starting and a greater fuel flow range over which resonant combustion will occur.

(4) "A contracting burner exhaust results in a lower rate of change of thrust with respect to average burner head pressure, poorer starting, and a lower fuel flow range for resonant combustion than does an expanding burner exhaust.

(5) "Use of an expanding burner exhaust results in a greater fuel flow range for resonant combustion than with a constant area exhaust, but does not significantly affect thrust versus average head pressure.

(6) "Burner thrust versus average head pressure appears to be not nearly so sensitive to burner length and exhaust configuration as it is to direction of inlets. On the other hand, ease of starting and the range of fuel flow to support resonant combustion appear to be more dependent on burner length and exhaust configuration than on inlet direction.

(7) "The average burner head pressure required to produce a given thrust is a function of inlet tube direction, and can vary widely from one direction of inlet tube to another.

(8) "The optimum location of the fuel nozzle exit is in the plane of the inlet tube entrance.

(9) "In general, performance decreases severely as the inlet tube penetration into the combustion chamber increases and as the inlet tube length is reduced below some optimum value (for a given burner).

(10) "The particular shape of the curve of burner head pressure vs radial distance from the burner axis appears to be set by inlet tube characteristics, and appears similar to (and therefore predictable from) the shape of the curve obtained when air alone is blown through the fuel nozzles and there is no combustion.

(11) "For a given burner length (which for practical purposes would certainly be as short as possible), resonant burner performance is highly sensitive to inlet tube direction, length, degree of penetration into the combustion chamber, and exhaust configuration, and these areas should eventually be explored further as a means of optimizing burner performance.

(12) "While recognizing the necessity for an expanded future program of static burner testing to optimize performance and basic design parameters, it is recommended that a shrouded 100-inlet combustor now be built and tested to verify that the gap between a static burner with a small number of inlets and a shrouded burner with a much greater number of smaller inlets can be bridged in a practical manner".

3.2 Connected-Pipe Tests and Results

As noted in paragraph 2.4.2 of this report, a multiple-inlet shrouded burner was constructed for connected-pipe tests based on the results and conclusions obtained from the static burner testing. Early attempts to use liquid fuel with this burner indicated liquid fuel system requirements to be fairly incompatible with gaseous fuel system requirements. This necessitated that liquid fuel experimentation be put aside temporarily in favor of determining optimized burner parameters with gaseous fuel, and returning to liquid fuel testing toward the end of the program if time permitted.

Burner characteristics were investigated over a range of shroud overhang lengths (8-3/4", 6-3/4", 5", 4-1/4", and 3-1/2"), for a range of ram air flows within each of which a range of fuel flow from lean-out to rich-out (or near rich-out) was investigated. The results permit an evaluation of thrust, pressures and temperatures, ram air flow effects, fuel consumption, combustion efficiency, resonant frequency, combustor shroud overhang effects, and combustor configuration. For purposes of continuity and ease of data comparison, the data are presented in accordance with the method used in Reference (2), using subscripts identified in Figure (23).

3.2.1 Thrust

Thrust was measured with various ram air flow rates and fuel flow rates at the five different nozzle overhang lengths, first with only ram air flowing, and then with the engine operating (combustion exhaust gases

flowing out the engine exit in addition to ram air). The relationship of thrust to engine nozzle exit pressure is shown in Figure (14), with a total of 174 test points (87 with ram air only and 87 with combustion) superimposed on a theoretical curve (see Reference 2 for derivation). Although almost all of the "cold" points lie above the theoretical curve, indicating error either in the measuring of thrust or of pressure, the "hot" points (where the burner was operating) showed relatively good correlation.

The gain in thrust ("hot" thrust minus "cold" thrust) is the thrust gain imparted by the burner, and is shown as a function of fuel flow rate at various nozzle overhang lengths and various air flow rates in Figures (24) through (28). The data of Figures (24) through (28) show a lower thrust gain than actually existed. This is because the air flow was reduced by as much as 20% when burning began, giving a lower effective thrust due to air flow and consequently a higher value of thrust gain than is obtained from calculating "hot" thrust minus "cold" thrust. From the figures it is seen that the thrust-fuel flow relationship at a given air flow is about the same for all the nozzle overhang lengths tested. The range of fuel flows over which the burner would resonate is seen to be largest at 6-3/4" nozzle overhang, to be slightly smaller at 5-3/4" overhang, and to decrease fairly rapidly as nozzle overhang is reduced to 5", 4-1/4", and 3-1/2".

3.2.2 Pressures and Temperatures

Pressures and temperatures upstream of the burner and at the exhaust

exit were measured on each run. The correlation of measured pressure with measured thrust as seen in Figure (14) is evidence as to the accuracy of the exhaust pressure data, which were obtained at a single point in the exhaust rather than by a wake traverse. The measured "hot" exhaust temperature data, on the other hand, appear to be considerably in error, based on the theoretical plot of Figure (16). Here the measured weight flows are plotted versus measured pressures, superimposed on a set of theoretical curves for several temperatures. The facing page, Figure (15), shows the data points obtained in the Phase I work and reported in Reference (2). These theoretical curves, based on the derivation of Reference (2), show the measured values of temperature to be too high. Since the exhaust temperature was measured at a single point rather than by a wake traverse, it is assumed that the data are in error, and the theoretical values of temperature as obtained from Figure (16) will be used to complete the analysis of the data.

Pressure Loss Coefficient and Temperature Rise Ratio versus air flow are shown in Figure (20). (The facing page, Figure (19), shows the data points obtained in the Phase I work and reported in Reference (2)). In order to improve the legibility of Figure (20), the plotted data are reduced to a minimum. A complete set of data is plotted for the 6-3/4" nozzle overhang, but the 4-1/4" nozzle overhang data are eliminated and the data shown for 8-3/4", 5", and 3-1/2" overhang is limited to that obtained with maximum and minimum fuel flow at maximum and minimum air flow. Three conclusions are derived from the curves of Pressure Loss Coefficient:

(1) the 6-3/4" nozzle overhang is the best of those tested from a pressure loss standpoint, since the increase of pressure loss when the burner is started is less than with any other overhang, and in a number of cases pressure loss is decreased;

(2) as nozzle overhang is decreased progressively from 6-3/4", the rise in pressure loss when burning is started becomes progressively greater;

(3) although fuel flow rates are not indicated on the curves, the smaller pressure loss increases occur with the minimum fuel flow rates at each overhang length and at each approximate air flow rate.

The curves of Temperature Rise Ratio are included for continuity, although these curves have limited experimental significance since they are not actually test data. As was previously noted, the test temperature data are believed to be considerably in error. The $\frac{T_{t_4}}{T_{t_2}}$ points plotted in Figure (20) are theoretical values obtained from the plot of Figure (16), from a knowledge of the pressures and weight flow rates during the tests. However, this was the method used in obtaining the Phase I curves (Fig. 19), so that a comparison is justified. As is evident from the two figures, the heat release capabilities of the inclined-inlet burner (Phase II) are about double that of the 90° inlet burner (Phase I).

High speed pressure measurements were made of the combustor and shroud pressures, and the test data were recorded on oscillograph tapes. Pressures

were measured at three shroud overhang lengths (8-3/4", 6-3/4", and 5"), at maximum and minimum air flow at each length, and at maximum and minimum fuel flow at each air flow. Plots of the results are shown in Figures (30) through (33). In Figure (30) is shown the maximum and minimum combustor pressure versus nozzle overhang length for the various flow conditions. Note the pronounced effect of air flow, fuel flow, and overhang length on combustor pressure. Here the 6-3/4" overhang length gives a striking pressure rise at low air flow and low air-fuel ratio; further, Figure (31) shows the shroud pressure to be only about 1 psi at this condition, indicating a combustor pressure rise of 3.5 psi. Note, also, that at this condition the combustor pressure varies by only about 1.2 psi and the shroud pressure by about 1.2 psi, but that the combustor pressure at its minimum is about 2.3 psi higher than the maximum shroud pressure. The jet-pumping effect of the fuel spray is indicated here by the ability of the combustor to re-charge with fresh air from a reservoir which is at a lower pressure, unless re-charging takes place at a different point in the shroud than where the pressure was measured, and where a standing wave may give a higher shroud pressure.

Figure (33) shows a plot of typical pressure graphs in the combustor and in the shroud for each of the conditions tested, and Figure (32), on the facing page, shows the values of the engine parameters which existed at the time of each condition. From these graphs, it is apparent that the high combustor pressure described above was unique to one or two conditions. However, the 6-3/4" overhang length is seen to have higher combustor pressure than shroud pressure (to re-charge from a reservoir at

lower pressure) under three of the four conditions tested. As is evident from Figure (33), the oscillograph results show the combustor pressure graph to be 180° out of phase with respect to the shroud pressure graph at all conditions tested. The oscillograph record showed the pressure graph as straight lines between maximum and minimum points. Had it been possible to increase tape speed, it is believed that the pressure graph would have appeared as a wave form; however it was not possible to increase oscillograph tape speed without compromising legibility of the traces.

3.2.3 Resonant Frequency and Starting

The shrouded burner would start resonating automatically upon the admission of fuel at air flows from .5 to 1.65 lbs per second. No attempt was made to test at lower air flow rates. As the nozzle overhang length was decreased below 6-3/4", the fuel flow rate required to start at any given air flow was increased. All resonance was within the range of 275 to 330 cps. On starting with a cold burner, with medium fuel flow rate, the initial frequency was 285 cps. Within about 5 seconds the burner would automatically shift to 292 cps and, within an additional 15 seconds it would shift to 310 cps. Sometimes an intermediate frequency of 300 cps would occur, making three distinct frequency shifts. Just prior to shifting, resonance would become unstable and the burner would sound as though it were missing every other firing; then with the following shift to the higher frequency, resonance would become strong and stable. It is concluded that these resonance shifts are due to burner expansion while

heating, since there is no further shift after the burner is heated unless fuel flow rate is varied widely. At very low fuel flow rate, initial resonance is at 275 cps, and at the highest fuel flow rate tested, final resonance is at 330 cps. In general, the final resonant frequency, increases slightly as fuel flow rate increases and increases slightly as overhang length decreases. These trends were verified by the oscillograph records made during the high-speed pressure measurements. As in previous resonant combustion work, it was noted that the burner automatically seeks a frequency at which it can resonate strongly and with stability.

3.2.4 Ram Air Flow

As would be expected, the effect of ram air flow on some burner performance characteristics is pronounced. Figures (24) through (28) show that the thrust gain due to burning increases nearly linearly with increasing air flow rate at any fuel flow rate. A cross plot of these curves, showing thrust gain versus air flow at a constant fuel flow rate, is shown in Figure (29) for each nozzle overhang length tested. The similarity of trend for each nozzle length, and the near linearity of thrust increase with air flow increase, is apparent. Note specifically that this thrust is the net thrust gain due to burning only, and is obtained by subtracting the thrust due to air flow from the total thrust measured with the burner operating. For this burner configuration, resonant burning could not be maintained at air flows in excess of the maximum shown.

The effect of air flow rate on pressure loss coefficient may be seen in Figure (20). For any of the overhang lengths shown, the "cold" pressure loss coefficient is approximately constant over the small range of air flow rates considered, which is reasonable to expect.

3.2.5 Fuel Flow

Consistent with the approximately linear increase in thrust gain with increase of air flow rate which was noted previously, Figure (18) shows specific fuel consumption to vary approximately inversely as air flow. This trend would probably be reversed after some optimum air flow rate has been reached. For this burner configuration, however, resonant burning could not be maintained above the maximum air flow rate shown, as noted previously.

Figures (24) through (28) show the effects of nozzle overhang length and air flow on lean-out and rich-out fuel flows. The resonating fuel flow range is reduced rapidly as nozzle (shroud) overhang length is decreased, with the range reduction occuring almost entirely on the lean-out end. The resonating fuel flow range does not show a clear trend with respect to air flow, except that when air flow is at the low end (less than $.034 \frac{\text{lbs}}{\text{sec-in}^2}$), the range is very much reduced.

3.2.6 Combustion Efficiency

Figure (22) shows fuel flow rate and combustion efficiency versus air flow rate, and the same curve from the Phase I work is shown on the facing page (Fig. 21) for ready comparison. Here the combustion efficiency is

derived by dividing theoretical fuel flow by the measured fuel flow, the theoretical fuel flow being obtained from Figure (17). While Figure (22) does not show thrust level, it permits a general comparison with the Phase I points, and the increase of efficiency with increase in air flow rate is readily seen. This increase in efficiency is discussed in Sections 3.2.4 and 3.2.5, and is evident also in Figures (18) and (29).

3.2.7 Combustor Shroud Overhang

Since combustor shroud overhang was one of the basic variables in the test work, evidences of its effects may be seen on several curves. Figure (20) shows the best overhang length from the standpoint of pressure loss coefficient tc be 6-3/4". At this overhang length, the pressure drop from the shroud inlet to the engine exit is in a number of cases reduced when the burner is operating. In almost all the other cases at this overhang length, the coefficient (computed from the measured data) increases slightly with burning. The 8-3/4" nozzle length appears to be about the same as the 6-3/4" length, perhaps not quite as good. When the overhang is reduced below 6-3/4" the coefficient increases with increasing severity as overhang length is reduced.

Figures (24) through (28) show the best length from tne standpoint of resonating fuel flow range to be 6-3/4". At 8-3/4" the range is slightly smaller, and at lengths below 6-3/4" the range becomes increasingly smaller as length is reduced.

The effect of overhang length on specific fuel consumption appears to be almost negligible, based on the plot of Figure (18). There appears a

trend towards higher fuel consumption as overhang length is decreased, but the air flows are not the same in each case, and efficiency has been shown to be affected by air flow rate. Figure (29) indicates the overhang length to have no apparent effect on specific fuel consumption.

3.2.8 Combustor Configuration

It would appear that the present combustor with inlets inclined 45° downstream is a superior combustor to the previous combustor with 90° inlets which was developed for the Phase I connected-pipe tests. Comparison of Figures (19) and (20) show the present configuration to provide a higher temperature rise ratio with a smaller rise, and often even a reduction, in pressure loss coefficient. Figures (21) and (22) show the present configuration to accommodate higher fuel flow rates than the previous configuration, and consequently a larger resonating fuel flow range. Figures (15) and (16) show the present configuration to achieve a higher exhaust pressure at a lower gas flow rate than the previous configuration, and therefore, according to Figure (14) a higher thrust. These improvements indicate the superiority of the present configuration, and again indicate the validity of static test results obtained with a small number of large inlets to predict performance trends of connected-pipe combustors with a large number of small inlets.

4. CONCLUSIONS

4.1 The slanting of the air inlets so as to direct the combustor exhaust blowback gases downstream was shown to be a decided improvement over the earlier configuration in which the blowback entered the shroud perpendicular to the by-pass passage-way.

4.2 The combustion chamber average pressure was quite low when operating under static conditions, as compared to representative valved and valveless pulsejets, but it increased with increasing (simulated) airspeed.

4.3 Starting with static operation, the combustion was shown to be quite complete as exhaust gas samples typically showed less than one percent combustibles.

4.4 The configuration investigated was marked by a contrasting combination of high combustion efficiency, and a mild pressure-gain mode of combustion, but with a thrust specific fuel consumption (Tsfc, lb fuel per hour per pound of thrust) which was more like that of a ramjet than a pulsejet. It is believed that the Tsfc would be improved with better matching between the shroud nozzle and the combustor.

4.5 The variation of shroud overhang length shows that there is an optimum length of shroud overhang beyond the end of the combustor, which infers that there is a tuning effect between the natural frequency of the combustor and the surrounding shroud.

4.6 General Conclusions

(1) It does not seem possible to give incontrovertible proof at this

stage of the art, but the evidence suggests that the benefit gained from the feature of submerging the air inlets is compromised by the need to reduce the length of the air inlets in order to submerge them. Whereas submerging the air inlets may have reduced the air inflow losses and contributed to a trend of improving performance with increasing airspeed, this is believed to have been counter-balanced by a reduction in combustion chamber pressure rise (and specific thrust) that may be associated with the reduction in relative length of inlets. A great reduction in air inlet length was necessary in order to make the inlets flush with the combustor exterior, and was accomplished only by using an unusually large number of inlets (30).

Although the configuration shows good starting characteristics (usually without requiring a blast of starting air), complete combustion, and reasonably good heat output with respect to volume, it is relatively low in thrust output, at low airspeeds.

(2) The results of the investigation strongly support the contention that resonant, valveless combustor configurations can be devised to be operationally compatible with ram shrouds which enclose them. However, best overall shrouded resonant combustor performance over the entire range from zero airspeed to high subsonic air speed, can be expected from a combustor with highest static (i.e., zero air speed) combustion chamber pressure (or specific thrust) and lowest static specific fuel consumption. This statement is dependent upon the requirement that the configurations must be arranged so that combustion exhaust gases do not interfere with

the inflow into the ram-shroud but rather are by-passed around the combustor within the shroud during the pressure-rise portion of the combustion cycle.

It is suggested that the best single combustor configuration for operation within a ram shroud will have several inlets (as many as six) that extend out of the combustor shell but are turned downstream, (a) so as to take advantage of the thrust from these so-called inlets and, (b) so the blowback from these inlets will help to induce flow through the ram shroud rather than blocking flow as would be the case if the inlets pointed upstream. However, the U-tube shaped engine is more fully developed for both static and for low-speed operation. Particular advantages are to be gained with this configuration in the case of twin combustors. It has been demonstrated with a variety of pulsejets that they can be operated 180° out of phase, i.e., when inflow is occuring in one combustor, the other one is discharging. When matched engines are enclosed in a common shroud, and operate 180° out of phase, both the inflow through the shroud diffuser and the jet efflux from the shroud nozzle is greatly smoothed. This should result in better performance of the ram shroud, as far as ram recovery and propulsive efficiency is concerned. An important by-product of pairing combustors is a reduction of the noise radiated at the fundamental or operating frequency of the combustors.

5. RECOMMENDATIONS FOR FUTURE INVESTIGATION

The following two types of resonant combustor configuration are recommended for further investigation in ram-shrouds:

1. A pair of U-shaped combustors in which the air inlet and tailpipe are faced in the same direction, as exemplified by those used in the "Pulse Reactors" being developed by this Contractor under U. S. Navy contract Noa(s) 59-6055c (Ref. 6), the pair of combustors to be operated 180° out of phase within a single shroud.

2. A resonant combustor in which there are a total of three to seven air inlets, with one small upstream facing inlet and the other inlets spaced around the combustion chamber with inlet tubes directed downstream within the ram-shroud.

5. REFERENCES

1. Lockwood, Raymond M., "A New Concept of Resonant Combustion". Hiller Aircraft Corporation - Advanced Research Division Report ARD-129 (1957).

2. Lockwood, R. M., "Investigation of a Resonant Combustor Concept, Phase I, Summary Report", Contract No. Nonr 2458(00). Hiller Aircraft Corporation - Advanced Research Division Report ARD-219 (1958).

3. Lockwood, R. M., "Proposal for Phase II Resonant Combustor Program", Contract No. Nonr 2458(00). Hiller Aircraft Corporation - Advanced Research Division Report ARD-215 (1958).

4. Heuer, G. E., and Lockwood, R. M., Progress Report No. 3, "Resonant Combustion Study Cortract No. Nonr 2458(00), Phase II. Hiller Aircraft Corporation - Advanced Research Division Report ARD-227 (1959).

5. Nichols, J. B., "An Energy Basis for Comparison of Performance of Combustion Chambers", Transactions of the A.S.M.E., Vol. 75, No. 1, January 1953, pp 29-34.

6. Lockwood, R. M., Sargent, E. R., and Beckett, J. E., "Development of a Thrust Augmented Valveless Pulsejet Lift-Propulsion System - Summary Report", Contract Noa(s) 59-6055c, Hiller Aircraft Corporation, Advanced Research Division Report ARD-256, 29 February 1960.

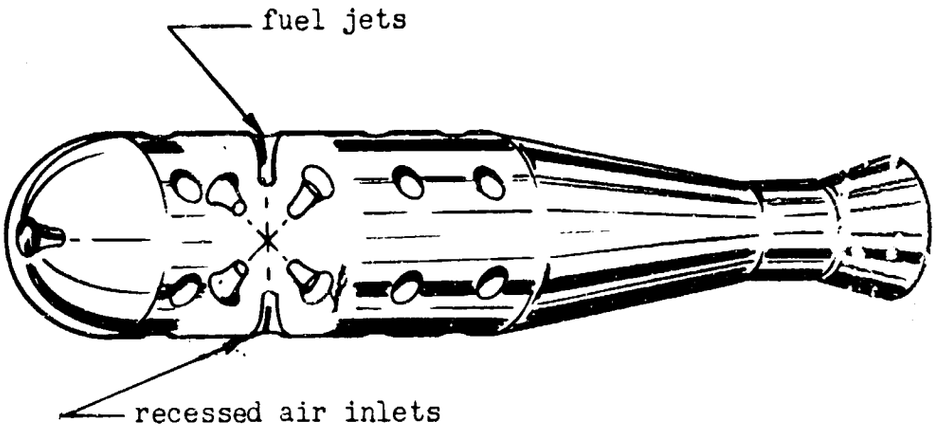

FIG. 1: INITIAL CONCEPTION OF RESONANT COMBUSTOR WITH MULTIPLE INJECTOR-TYPE AIR INLETS

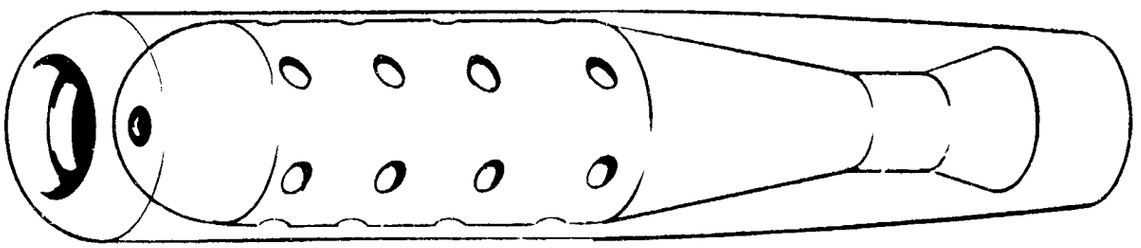

FIG. 2: INITIAL CONCEPTION OF MULTIPLE INJECTOR-TYPE AIR INLET RESONANT COMBUSTOR IN USE AS A DUCTED VALVELESS PULSEJET, RESONANT RAMJET, OR RESONANT COMBUSTOR IN A GAS TURBINE CYCLE

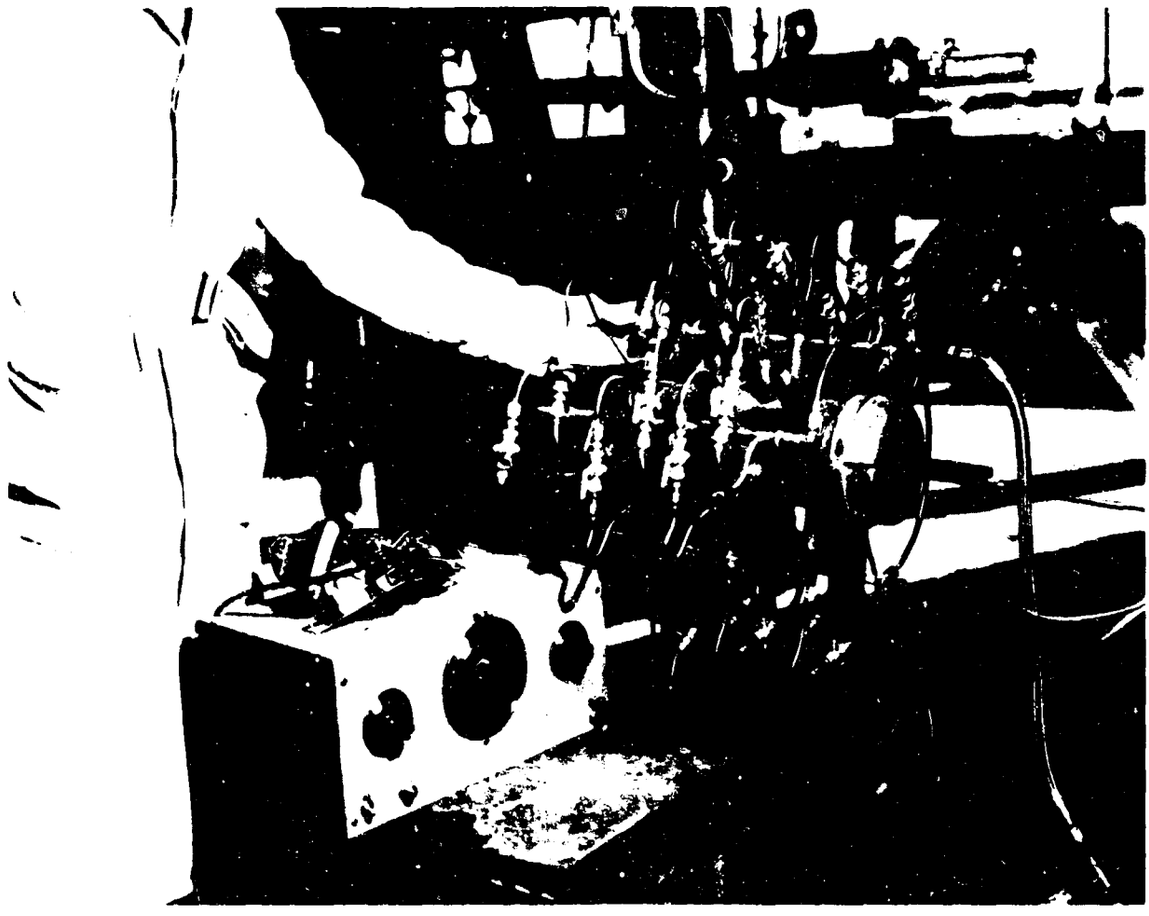

FIG. 3: MULTIPLE-INLET RESONANT COMBUSTOR. "BOILER-PLATE" MODEL IS USED TO TEST EFFECTS OF AIR INLET LENGTH AND LOCATION ON RESONANT COMBUSTION. AUDIO OSCILLATOR IS USED TO DETERMINE FUNDAMENTAL COMBUSTION FREQUENCY.

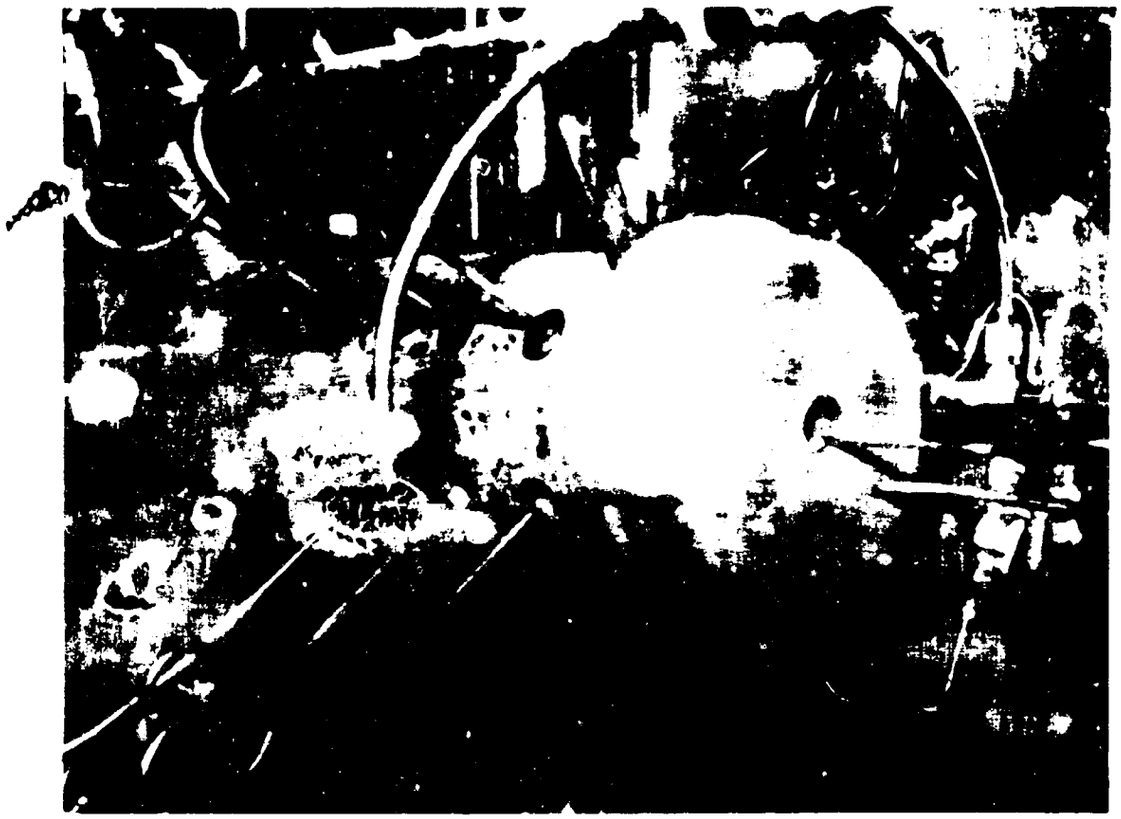

FIGURE 4: RESONANT COMBUSTOR WITH THIRTEEN AIR INLETS FLUSH WITH CHAMBER SURFACE. ONE-HALF INCH INSIDE DIAMETER AIR INLETS ARE ONE INCH LONG.

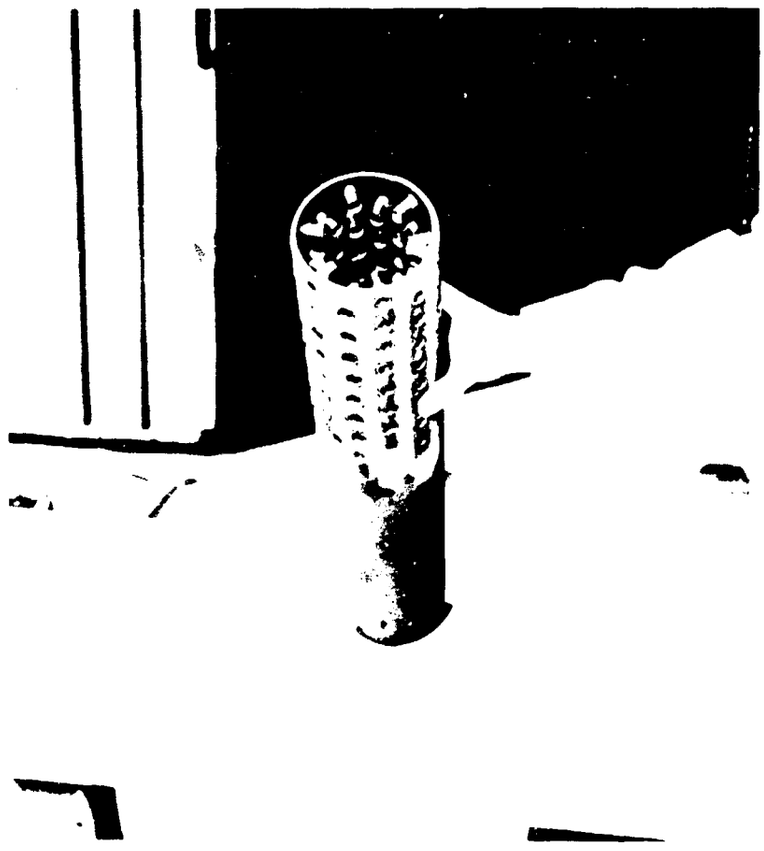

FIG. 5: FOUR-INCH DIAMETER RESONANT COMBUSTOR TUBE WITH 96 AIR INLETS, ONE INCH LONG BY 1/4 INCH DIAMETER, INSTALLED FLUSH WITH OUTER SURFACE.

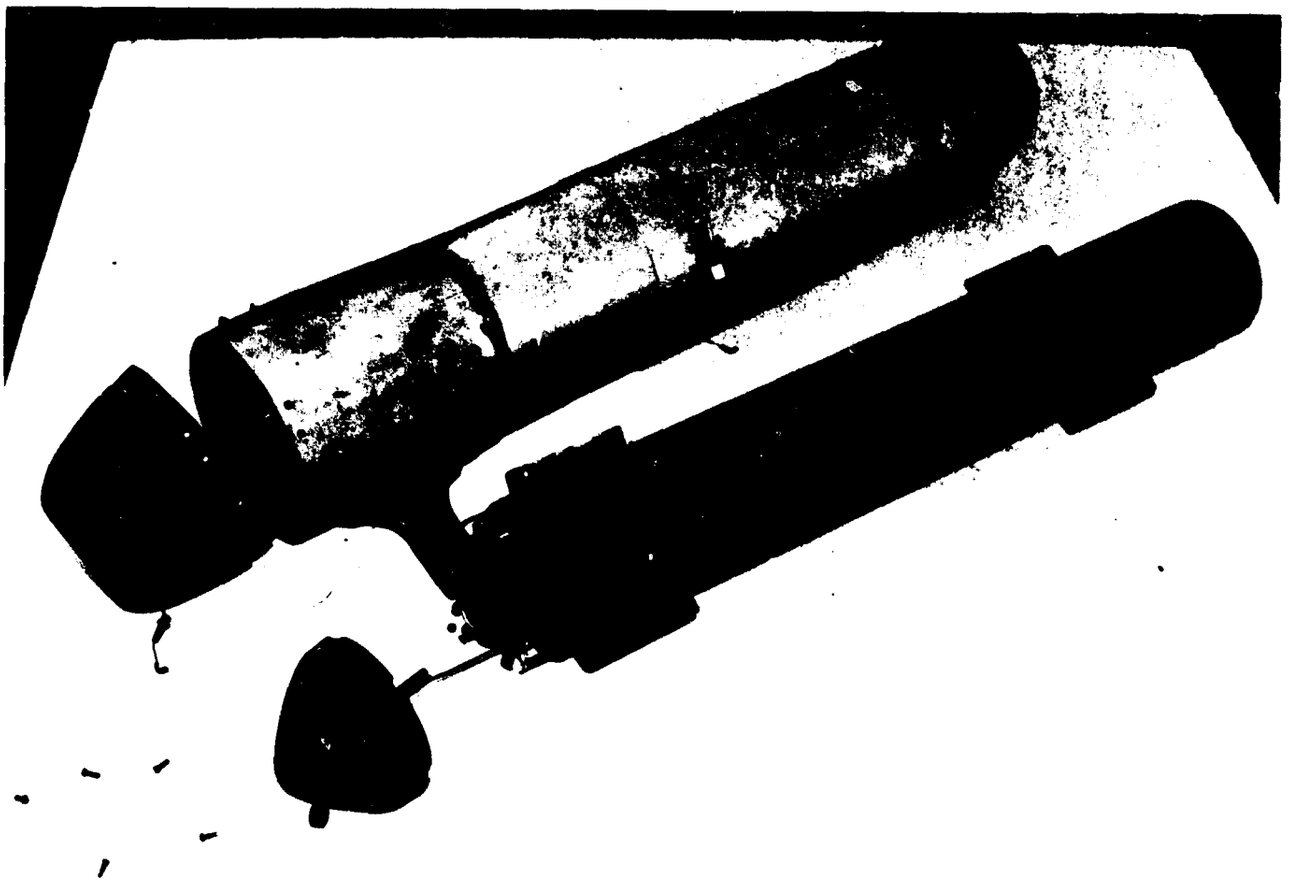

FIG. 6: 100-INLET RESONANT COMBUSTOR AND RAM SHROUD, DISASSEMBLED.

FIG. 7: RESONANT COMBUSTOR ASSEMBLED IN RAM SHROUD.

BASIC BURNER CROSS SECTION

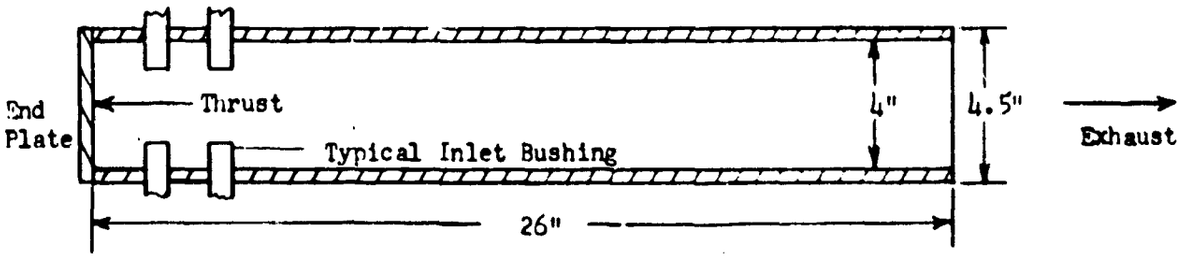

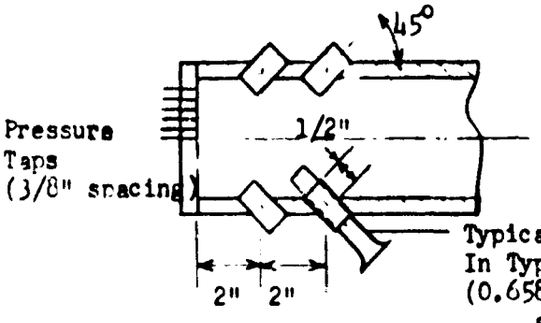

Typical Inlet Tube Set In Typical Inlet Bushing (0.658" I.D. x 3" L. for a) and b).)

a) Inlets Inclined 45° Downstream

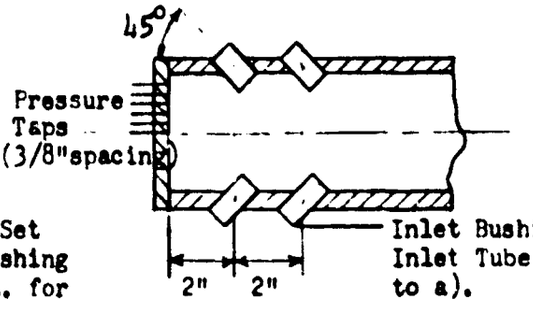

Inlet Bushing and Inlet Tube Identical to a).

b) Inlets Inclined 45° Upstream

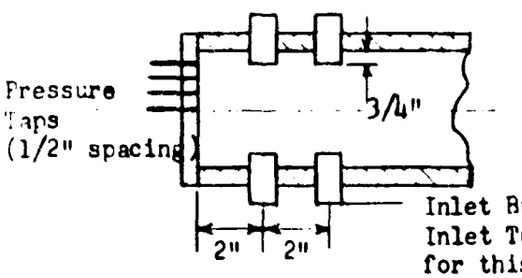

Inlet Bushing 1/2" Pipe x 1" L.
Inlet Tube 9/16" I.D. x 2-11/16 L. for this Burner

c) Inlets 90° To Burner ℄

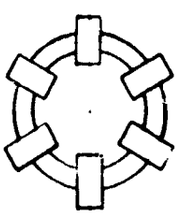

d) Typical Inlet Bushing Positions For a), b) and c): 2 Rows of 6 Inlets Each

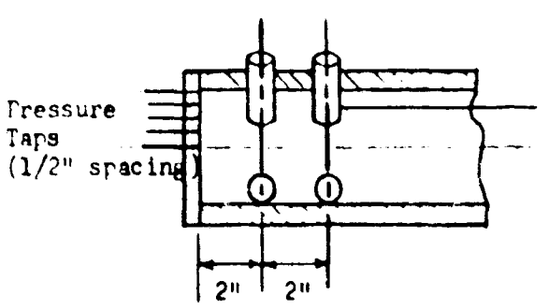

Inlet Bushing 3/4" I.D. x 1 1/4" L., Inlet Tube 0.658" I.D. x 3" L. For this Burner

e) Inlets Tangential To Burner ℄

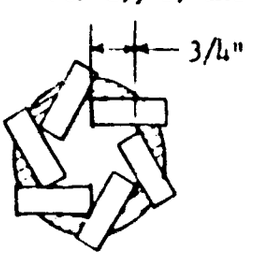

f) Inlet Bushing Positions for e): 2 Rows of 6 Inlets Each

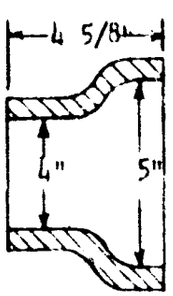

g) End Bell

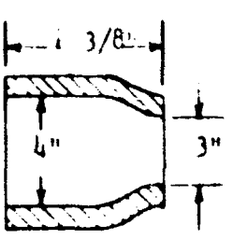

h) Reducer

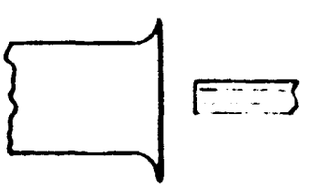

i) Fuel Spray Nozzle
All Inlets Size: .0335"

FIGURE 6: RESONANT BURNER CONFIGURATIONS

CONTRACT NO. AF 245E
EWA 3266
W.O. 310-001

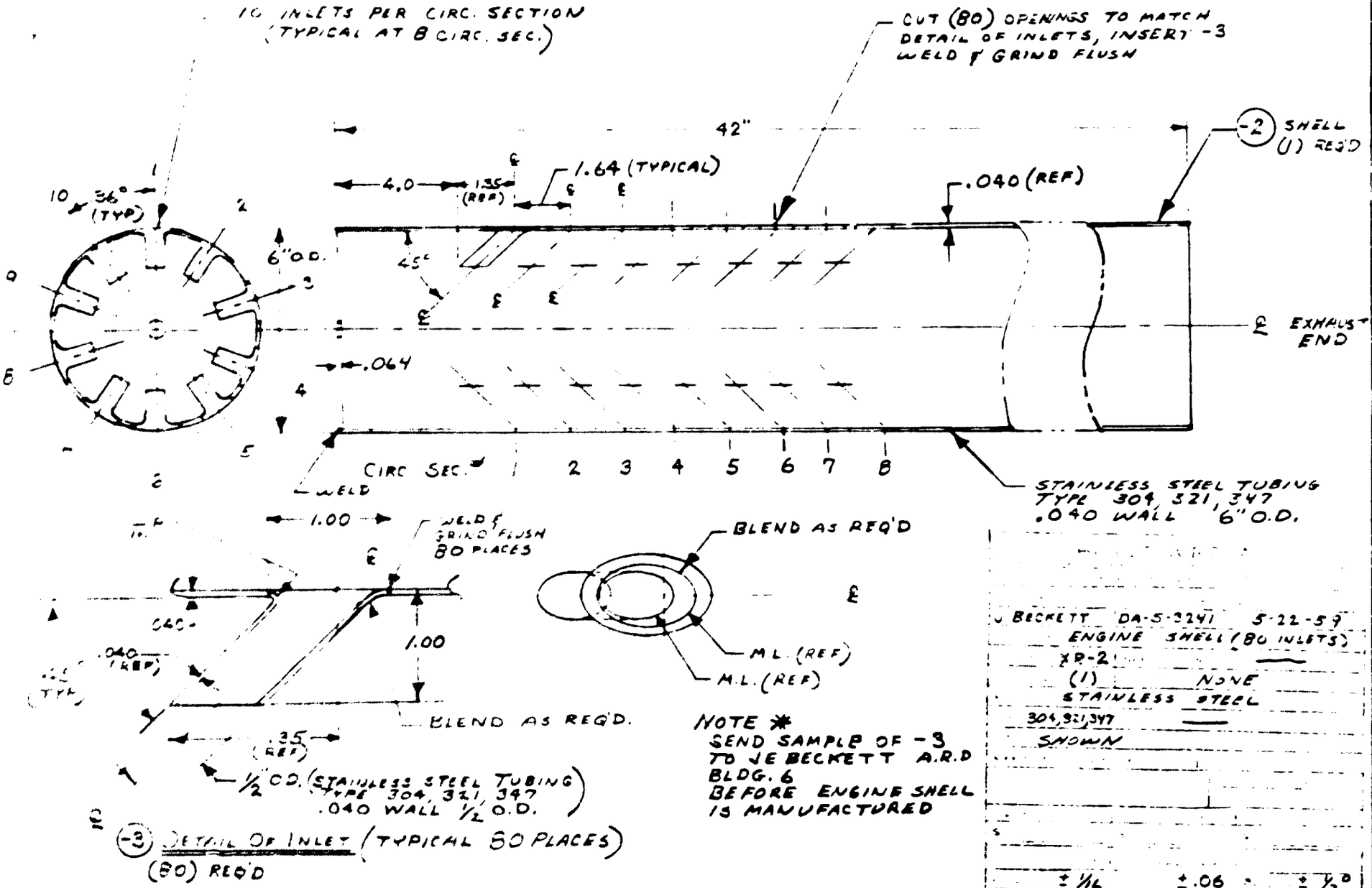

(-3) DETAIL OF INLET (TYPICAL 80 PLACES)
(80) REQ'D

NOTE *
SEND SAMPLE OF -3 TO JE BECKETT A.R.D BLDG. 6 BEFORE ENGINE SHELL IS MANUFACTURED

J. BECKETT DA-5-3241 5-22-59
ENGINE SHELL (80 INLETS)
XP-2
(1) NONE
STAINLESS STEEL
304, 321, 347
SHOWN

± 1/16 ± .06 ± 1/2°

FIG. 9. COMBUSTOR WITH SLANTED INLETS (SHOP SKETCH)

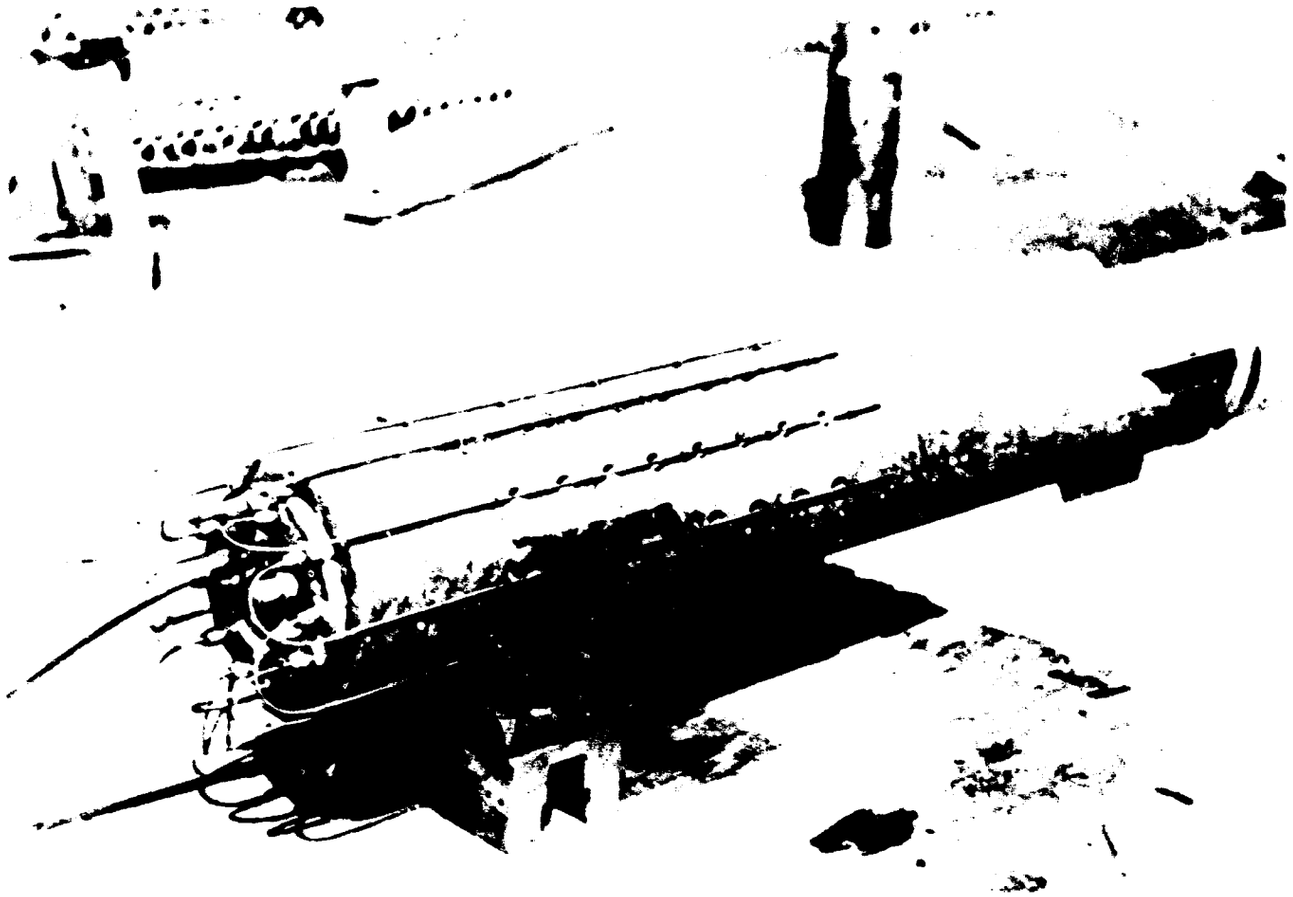

FIGURE 10: COMBUSTOR WITH SLANTED INLETS, (TEST ARTICLE)

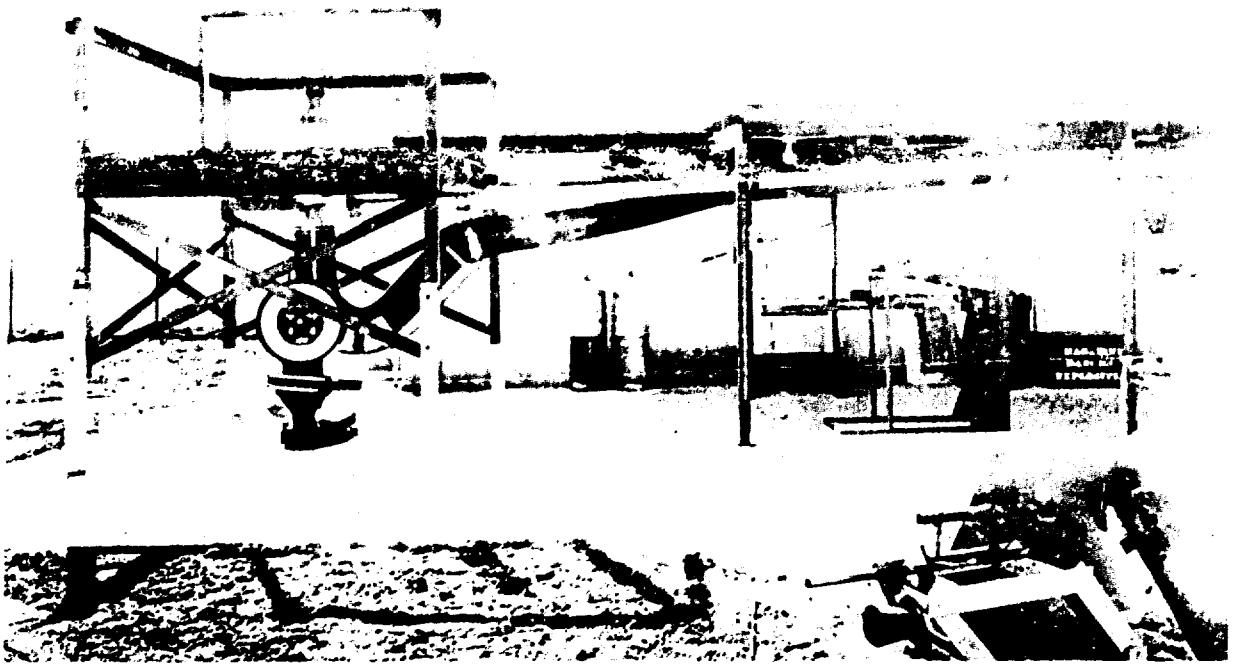

FIGURE 11: TEST STAND, SHOWING VERTICALLY-MOUNTED COMBUSTOR AND AIR SUPPLY PIPE FOR CONNECTED-PIPE TESTS

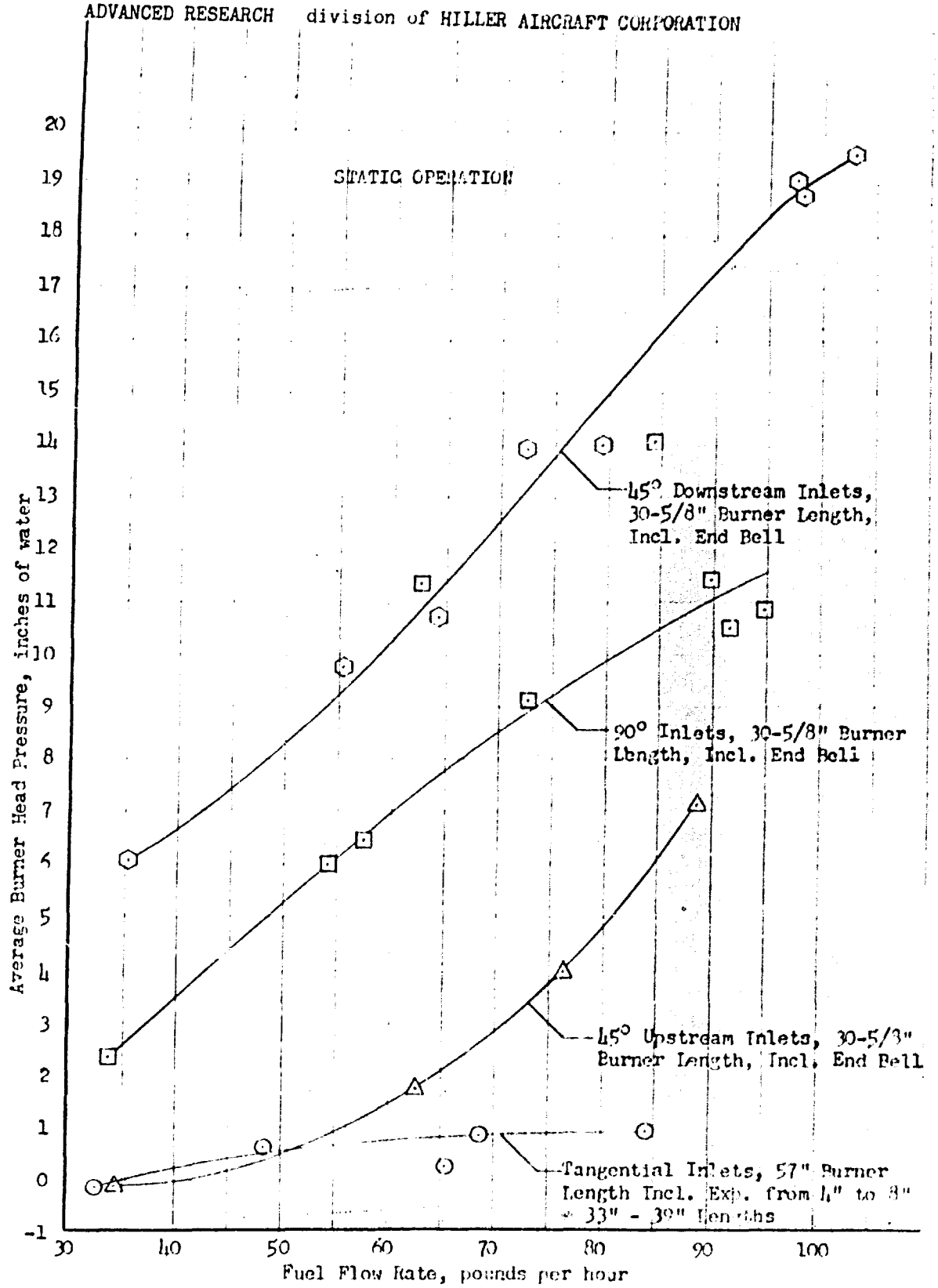

FIGURE 12: AVERAGE BURNER HEAD PRESSURE VS. FUEL FLOW RATE, VARIOUS INLET TUBE DIRECTIONS

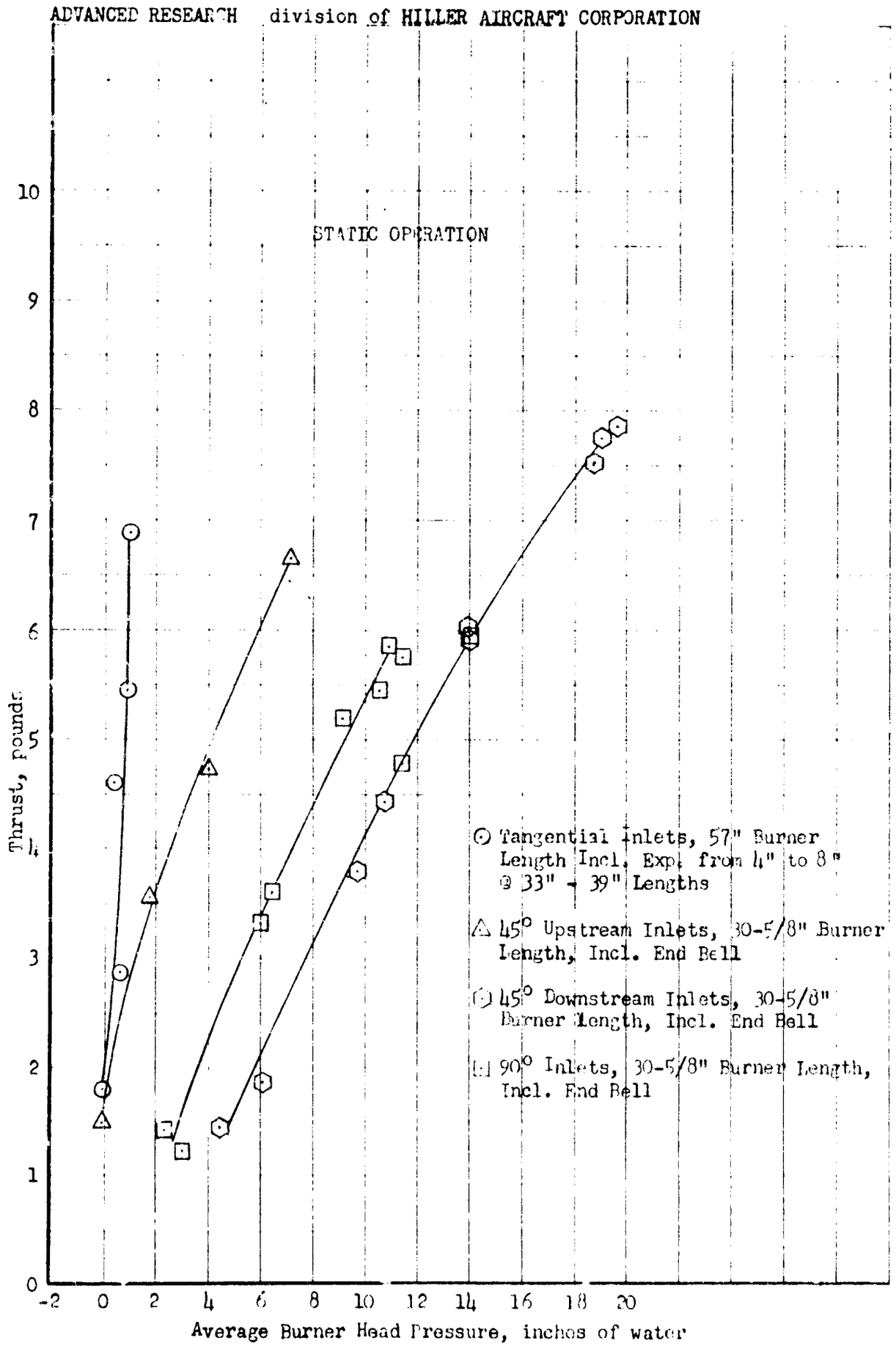

FIGURE 13: AVERAGE BURNER HEAD PRESSURE VS THRUST, VARIOUS INLET TUBE DIRECTIONS

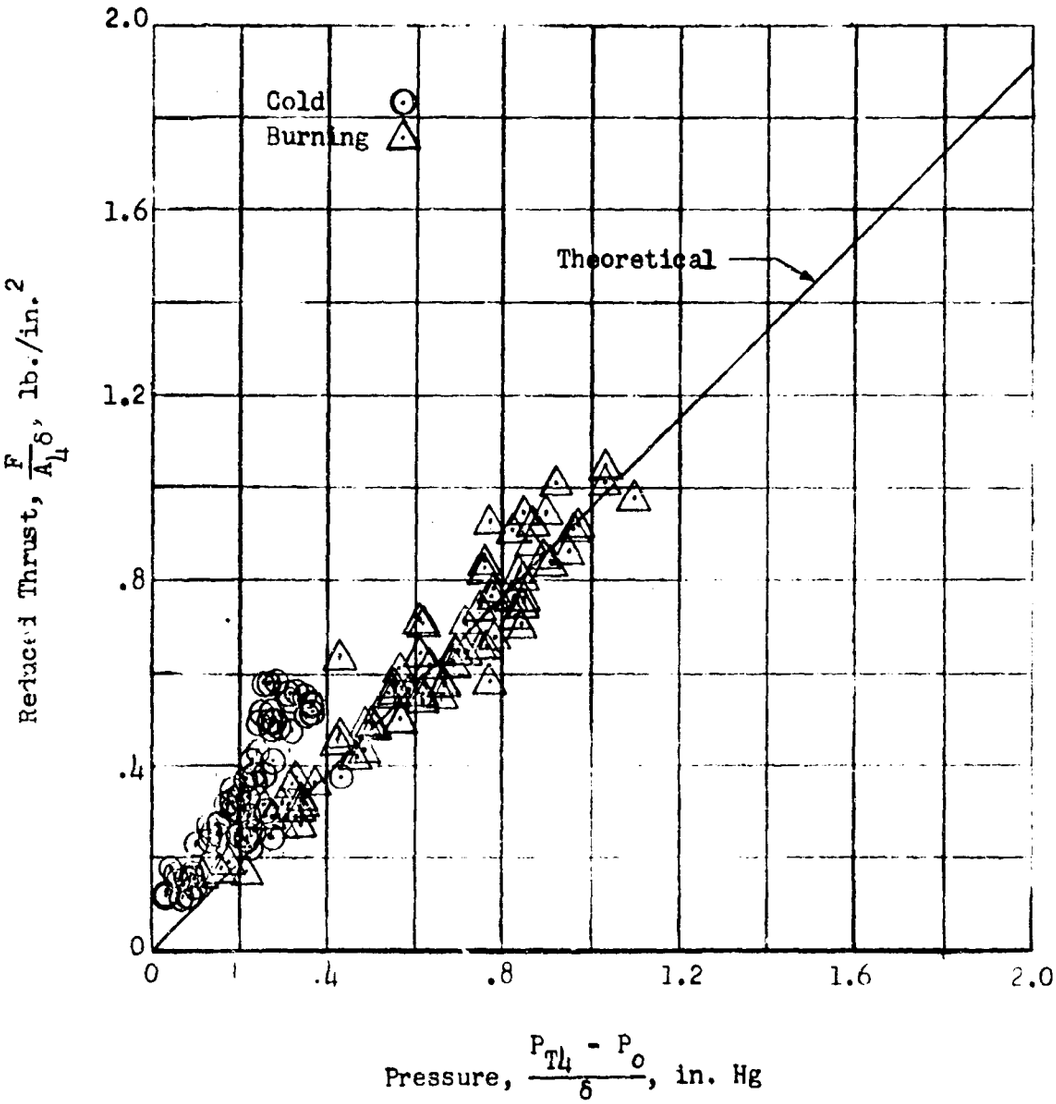
2.0
1.6
1.2
.8
.4
0
0
.4
.8
1.2
1.6
2.0
Cold
Burning
Theoretical
Reduced Thrust, $\frac{F}{A_4 \delta}$, lb./in.^{2}
Pressure, $\frac{P_{T4} - P_o}{\delta}$, in. Hg

FIGURE 14

PHASE I TEST DATA

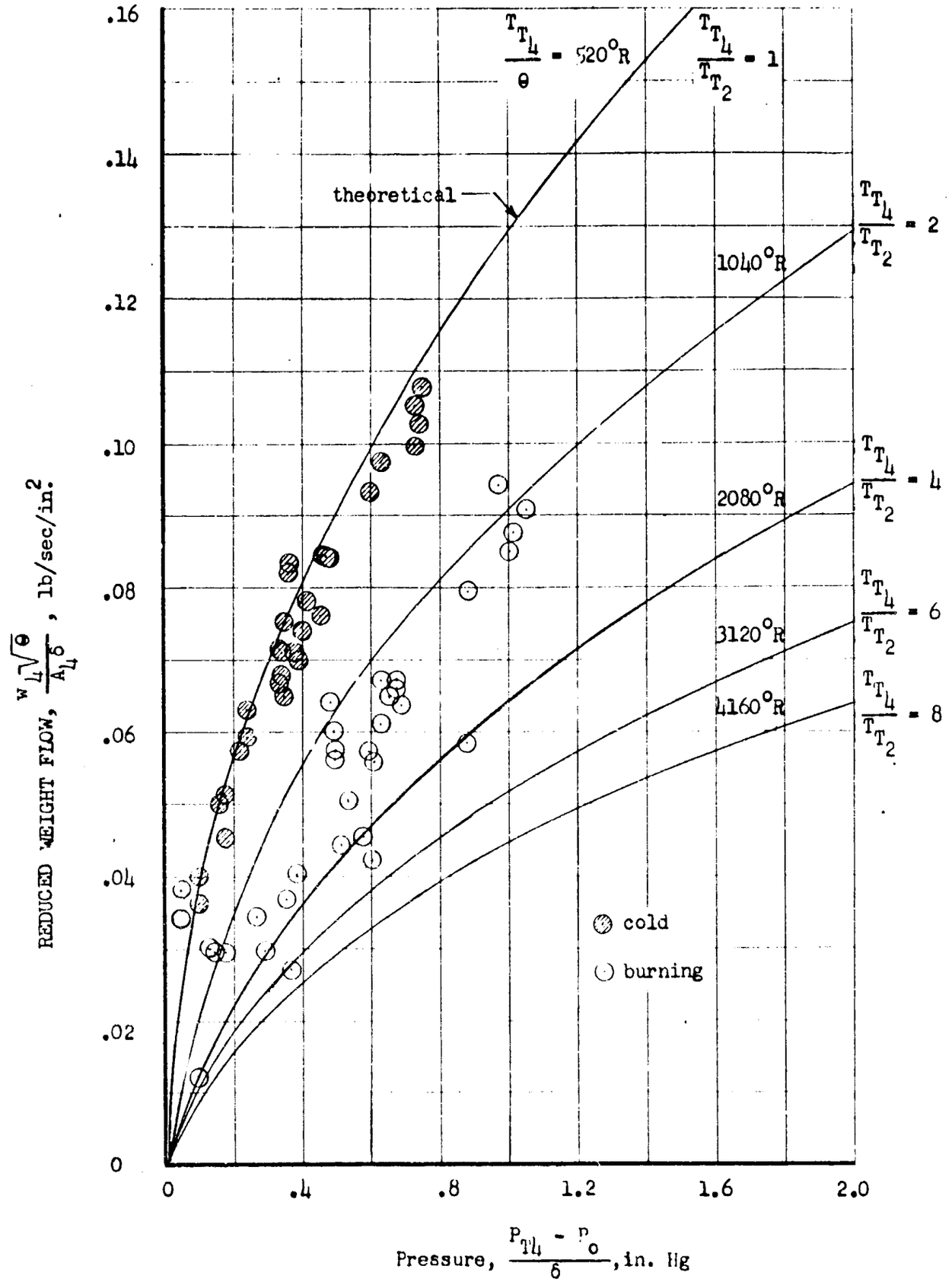

FIGURE 15

PHASE II TEST DATA

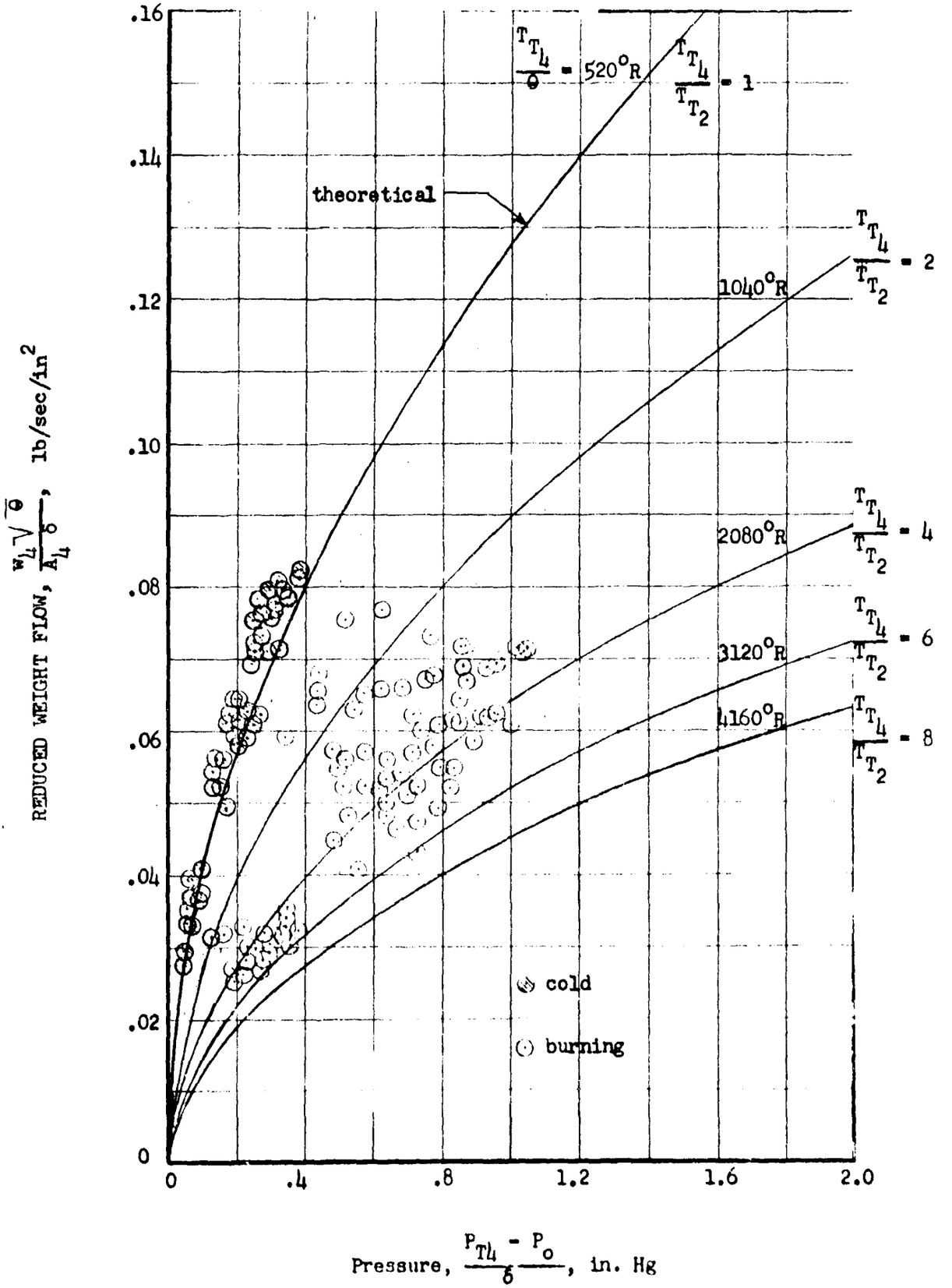

FIGURE 16

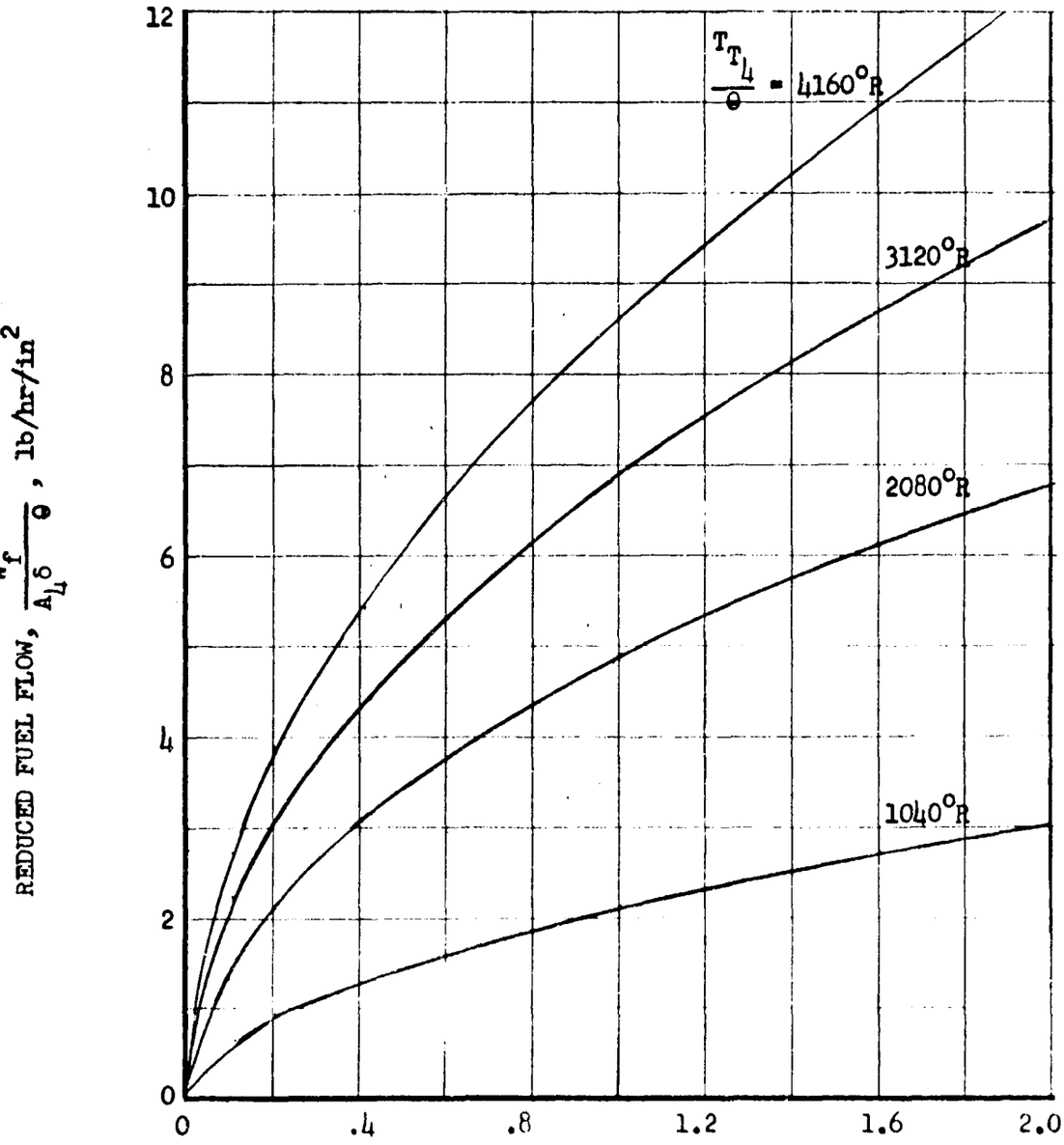
REDUCED FUEL FLOW, $\frac{W_f}{A_4 \delta} \theta$, lb/hr/in^2
$\frac{T_{T_4}}{\theta}$ = 4160°R
3120°R
2080°R
1040°R
0
2
4
6
8
10
12
0
.4
.8
1.2
1.6
2.0
Pressure, $\frac{P_{T_4} - P_o}{\delta}$, in. Hg

FIGURE 7

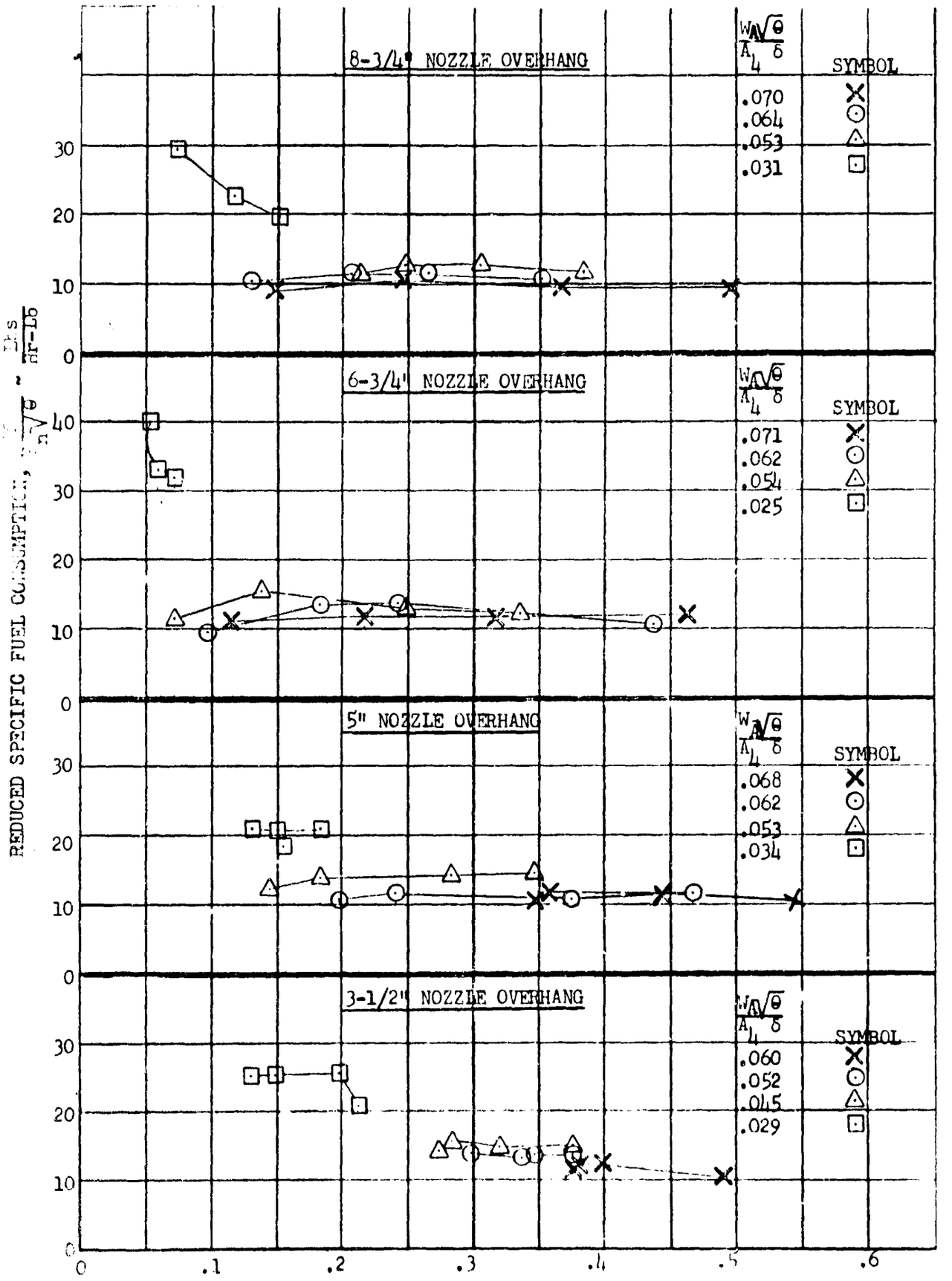
8-3/4" NOZZLE OVERHANG
6-3/4" NOZZLE OVERHANG
5" NOZZLE OVERHANG
3-1/2" NOZZLE OVERHANG
SYMBOL
.070
.064
.053
.031
.071
.062
.054
.025
.068
.062
.053
.034
.060
.052
.045
.029
0
10
20
30
40
.1
.2
.3
.4
.5
.6
REDUCED SPECIFIC FUEL CONSUMPTION
REDUCED NET THRUST, $\frac{F_n}{A_4 \delta}$ - Lbs.

FIGURE 18

PHASE I TEST DATA

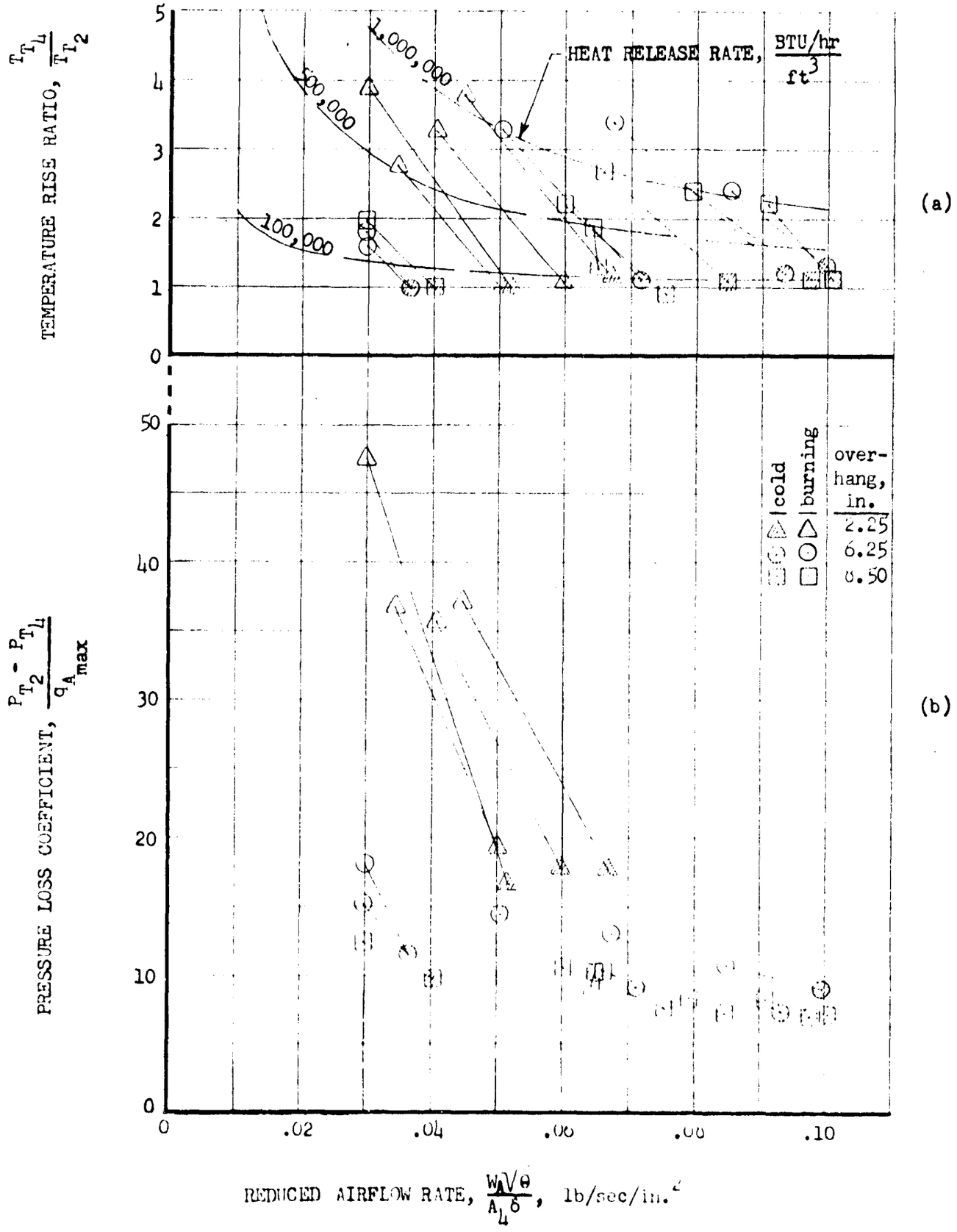

FIGURE 19

PHASE II TEST DATA

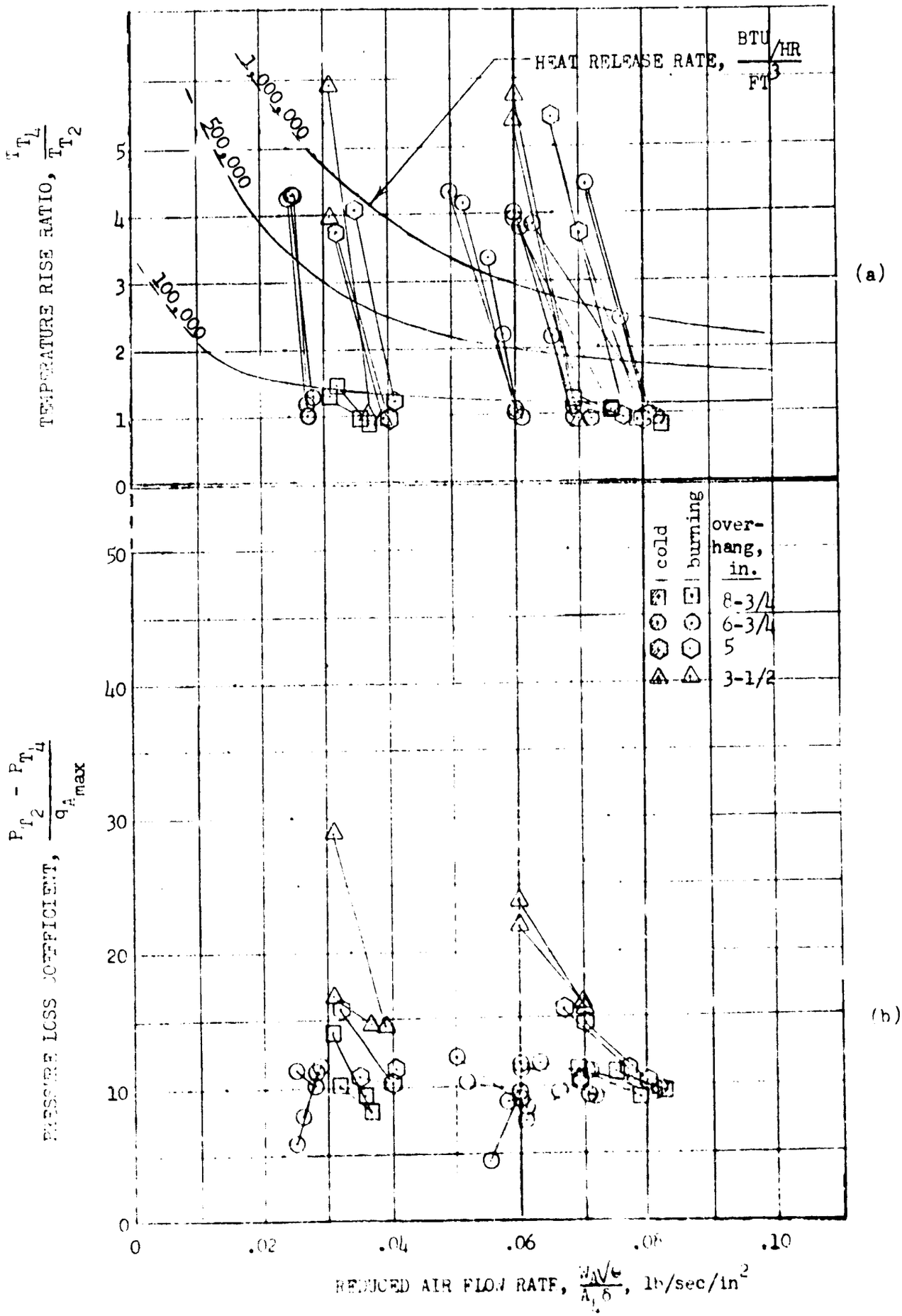

FIGURE 20

PHASE I TEST DATA

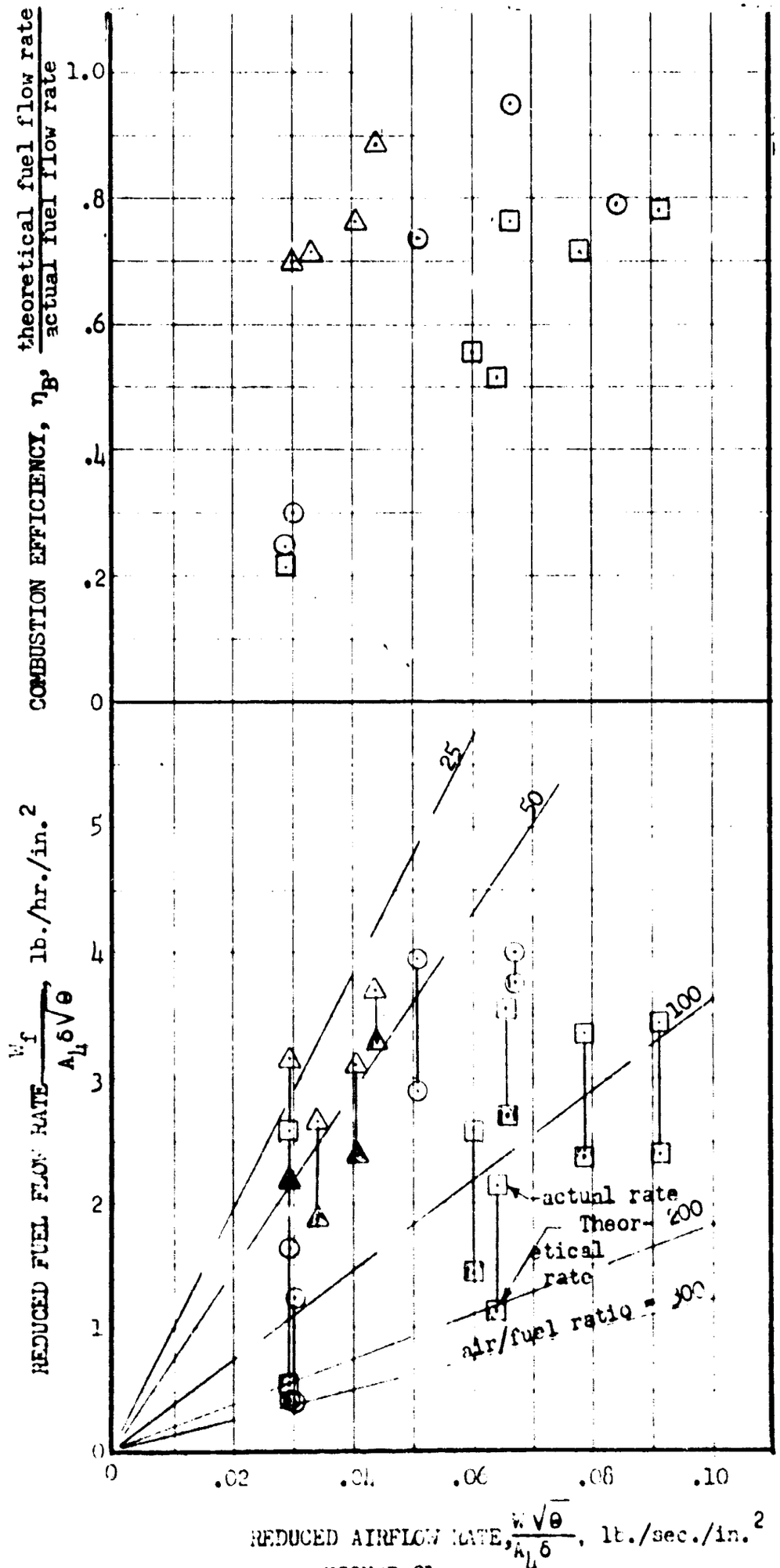

FIGURE 21

PHASE II - TEST DATA

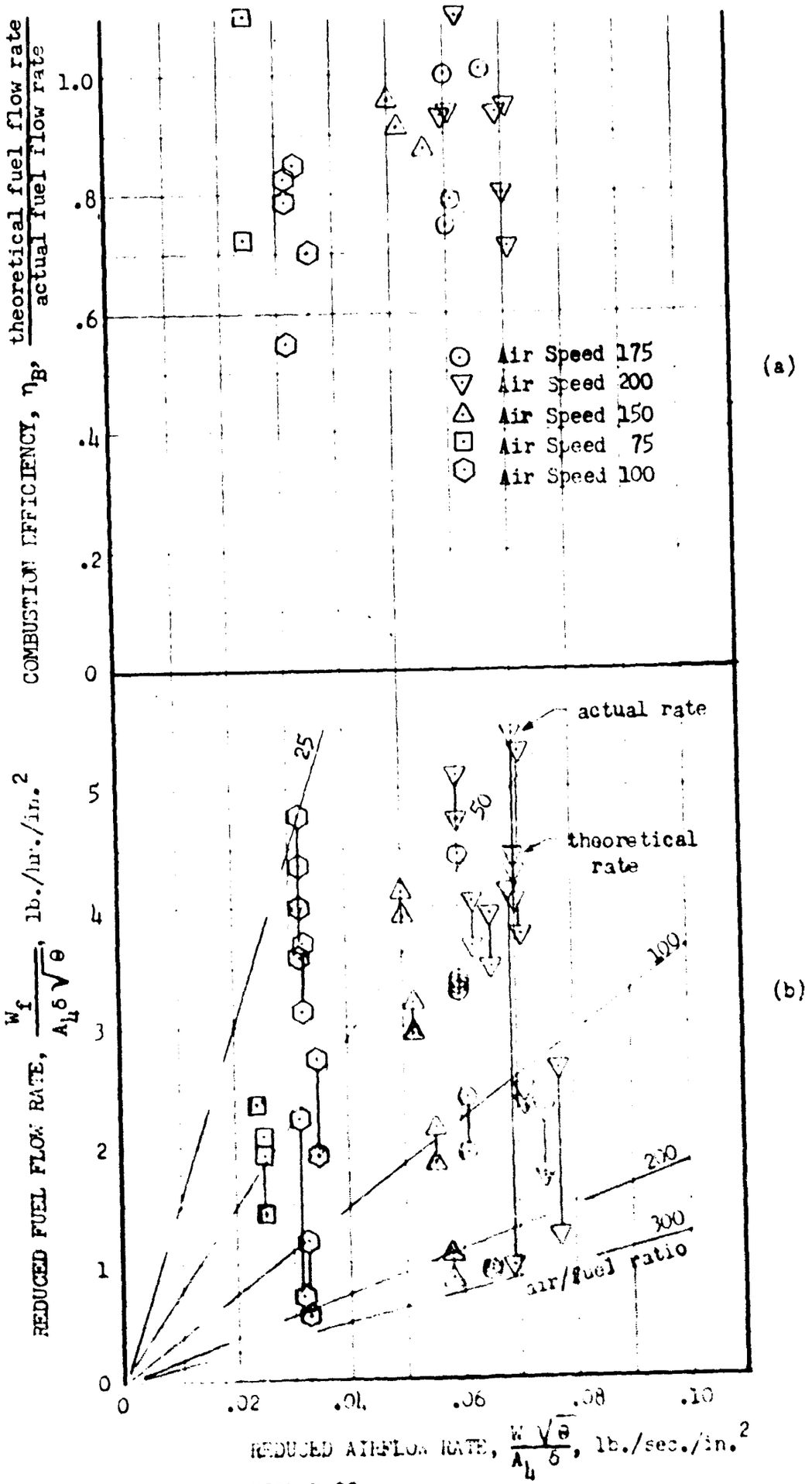

FIGURE 22

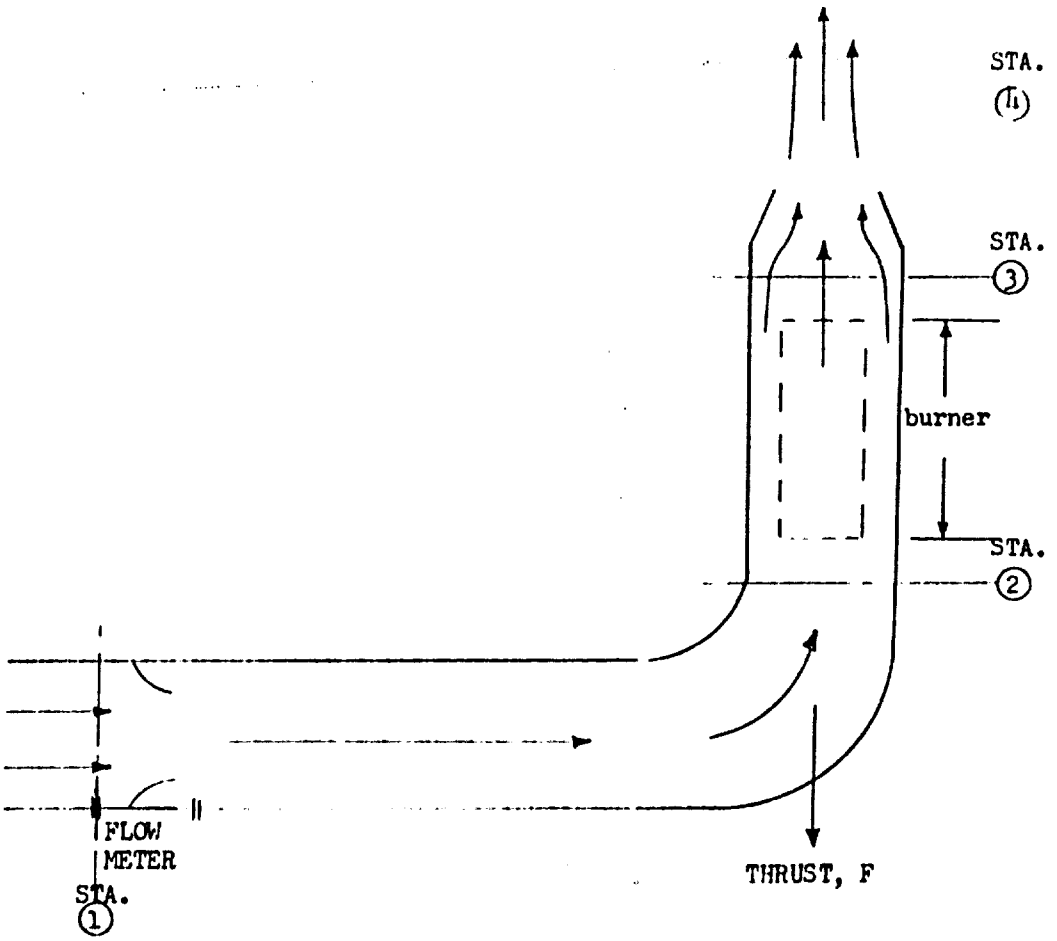

FIGURE 23: SKETCH OF TEST ARRANGEMENT

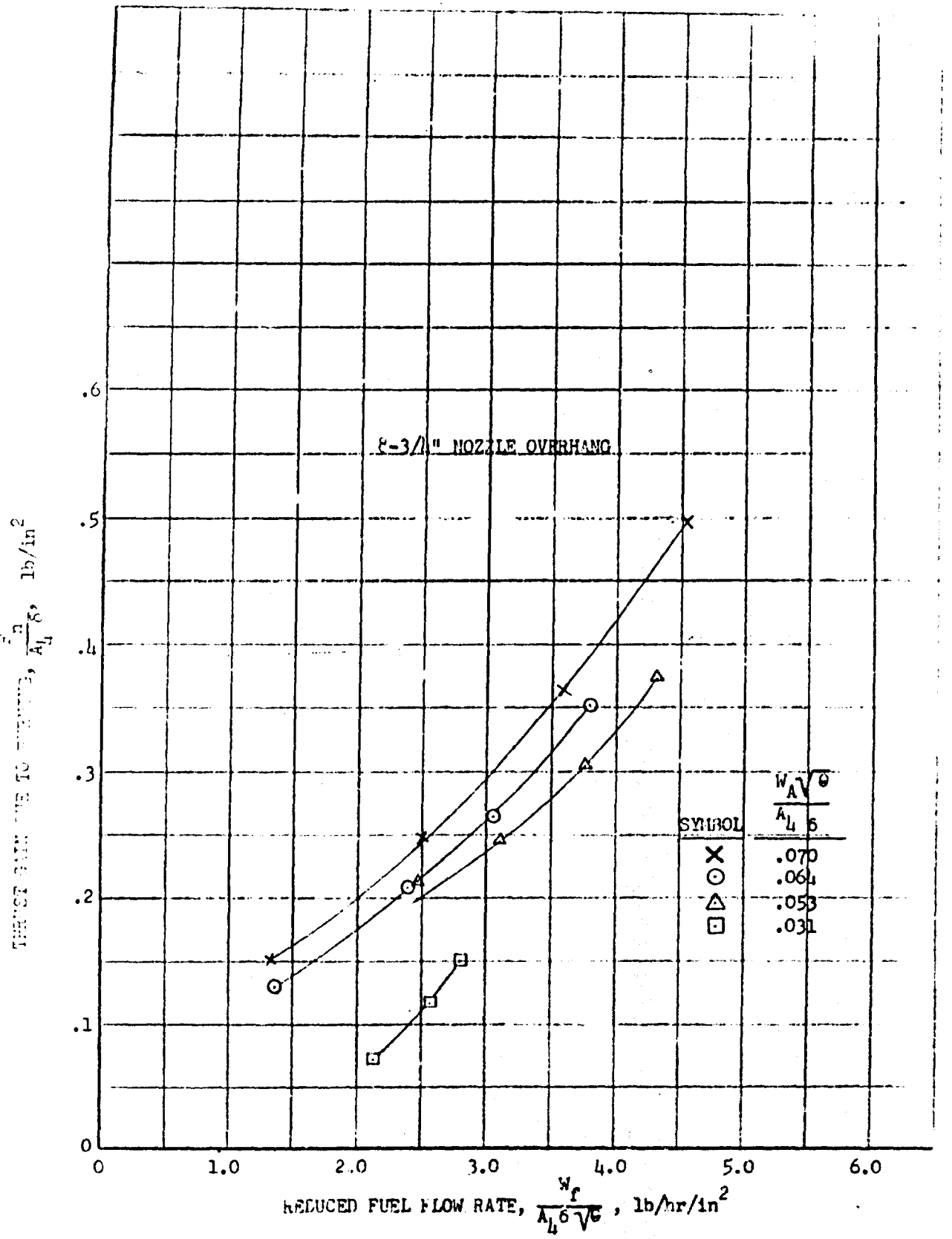

FIGURE 24

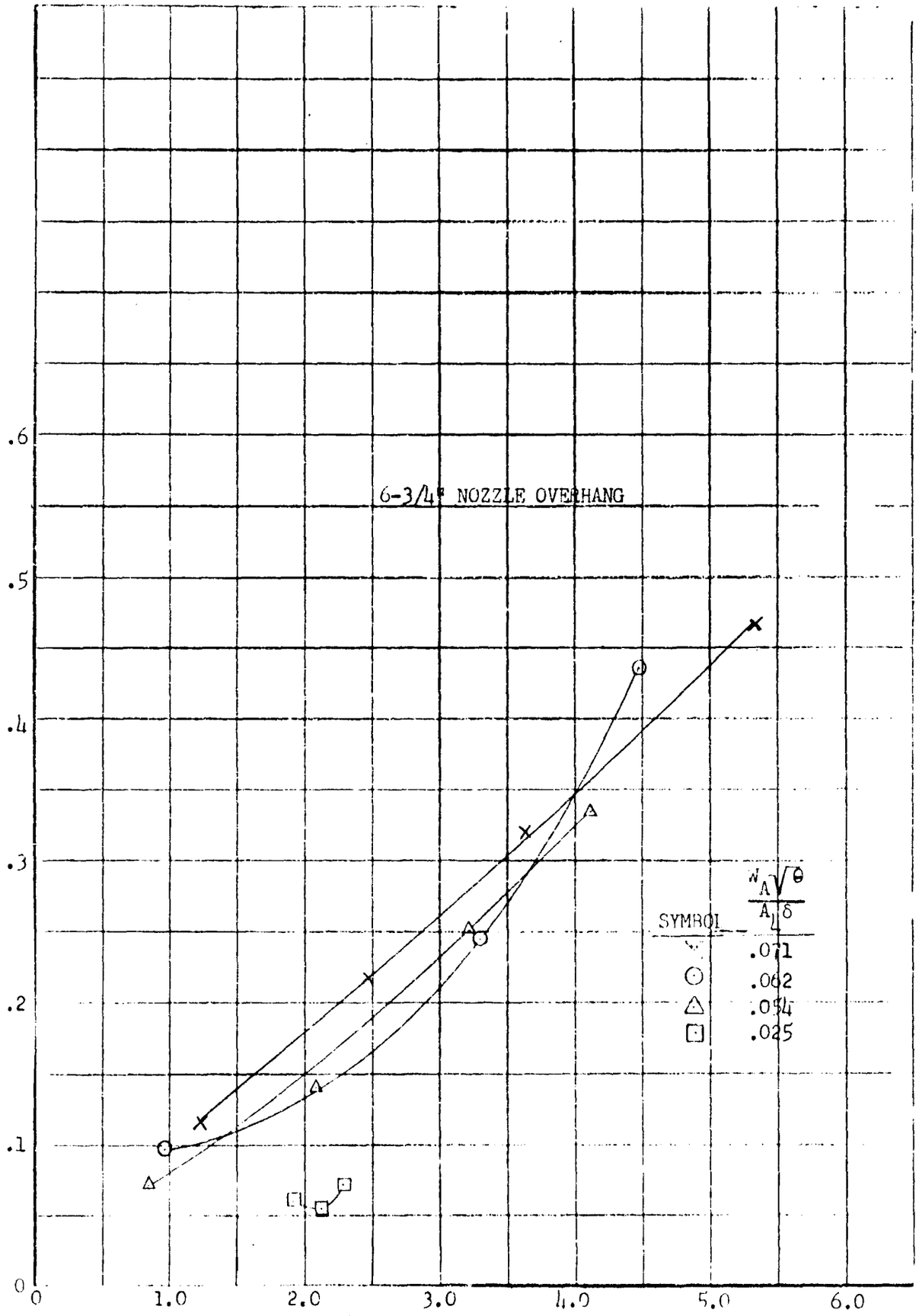

REDUCED FUEL FLOW RATE, $\frac{W_f}{A_4\delta\sqrt{\theta}}$, lb/hr/in^2

FIGURE 25

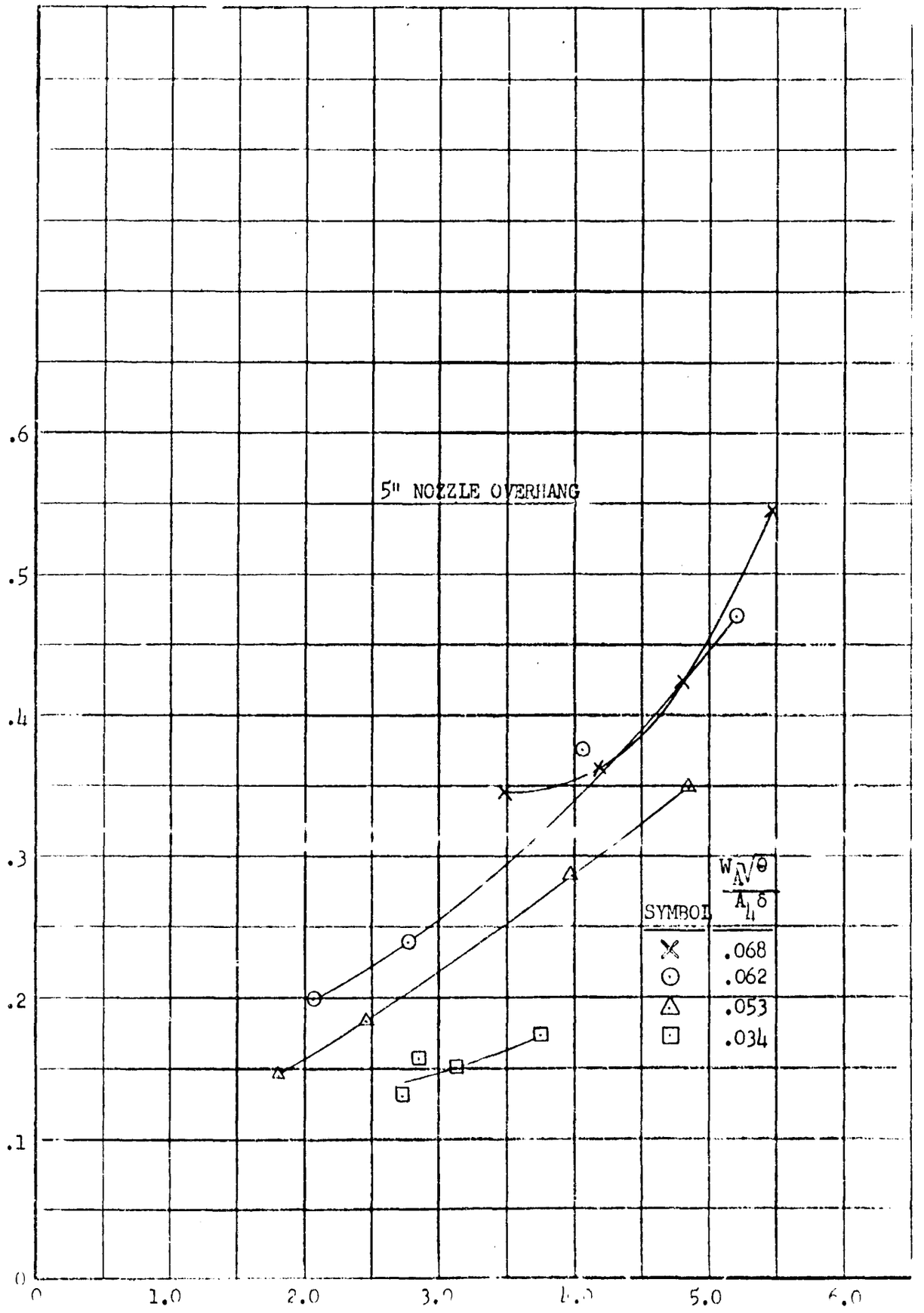
5" NOZZLE OVERHANG
SYMBOL
$\frac{W_A\sqrt{\theta}}{A_4\delta}$
.068
.062
.053
.034
0
.1
.2
.3
.4
.5
.6
1.0
2.0
3.0
4.0
5.0
6.0
REDUCED FUEL FLOW RATE, $\frac{W_f}{A_4\delta\sqrt{\theta}}$, lb/hr/in^2

FIGURE 26

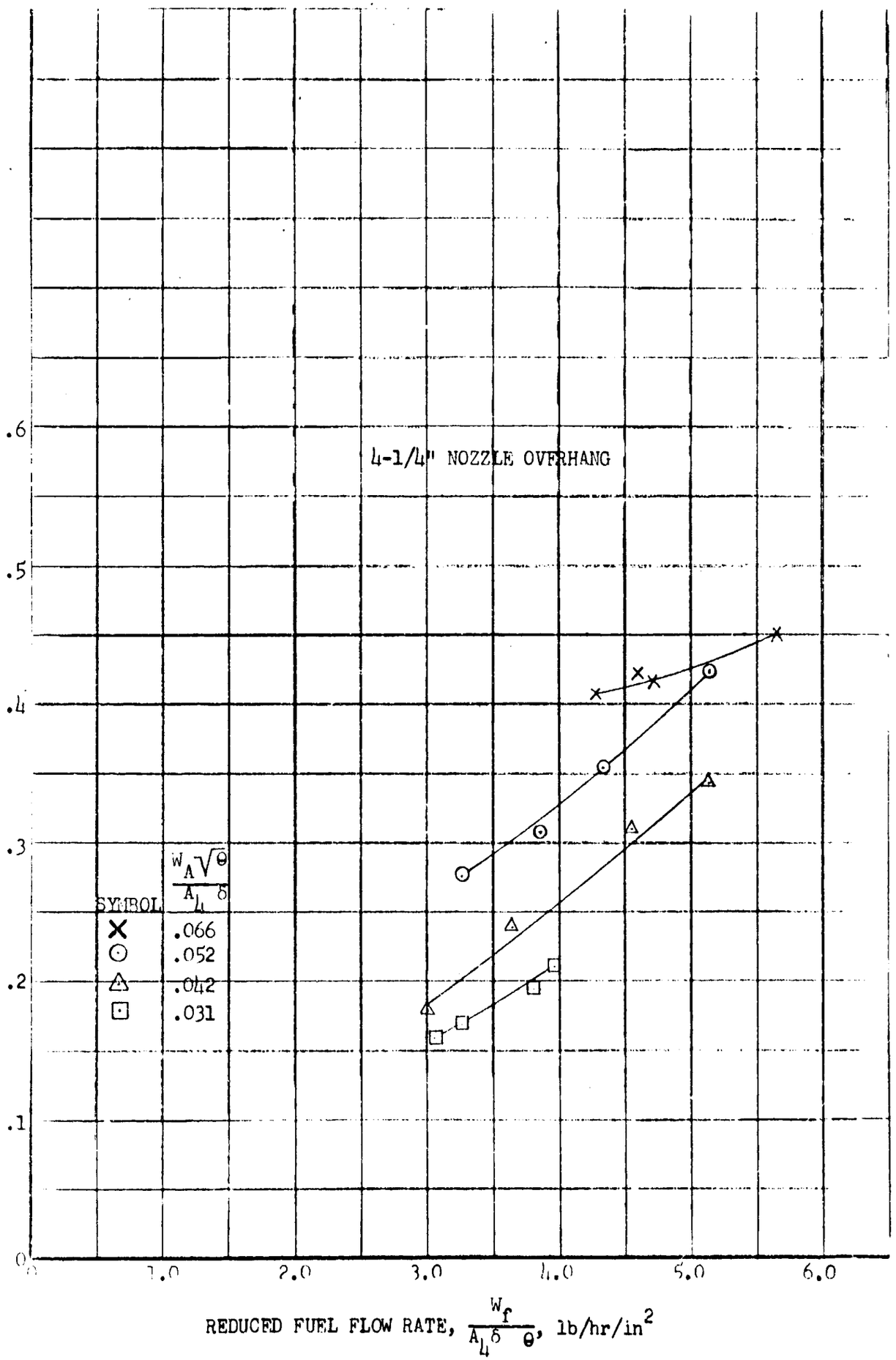
4-1/4" NOZZLE OVERHANG
SYMBOL
$\frac{W_A\sqrt{\theta}}{A_4\delta}$
.066
.052
.042
.031
0
.1
.2
.3
.4
.5
.6
1.0
2.0
3.0
4.0
5.0
6.0
THRUST GAIN DUE TO SPRING, $\frac{F_n}{A_4\delta}$, lb/in^2
REDUCED FUEL FLOW RATE, $\frac{W_f}{A_4\delta\ \theta}$, lb/hr/in^2

FIGURE 27

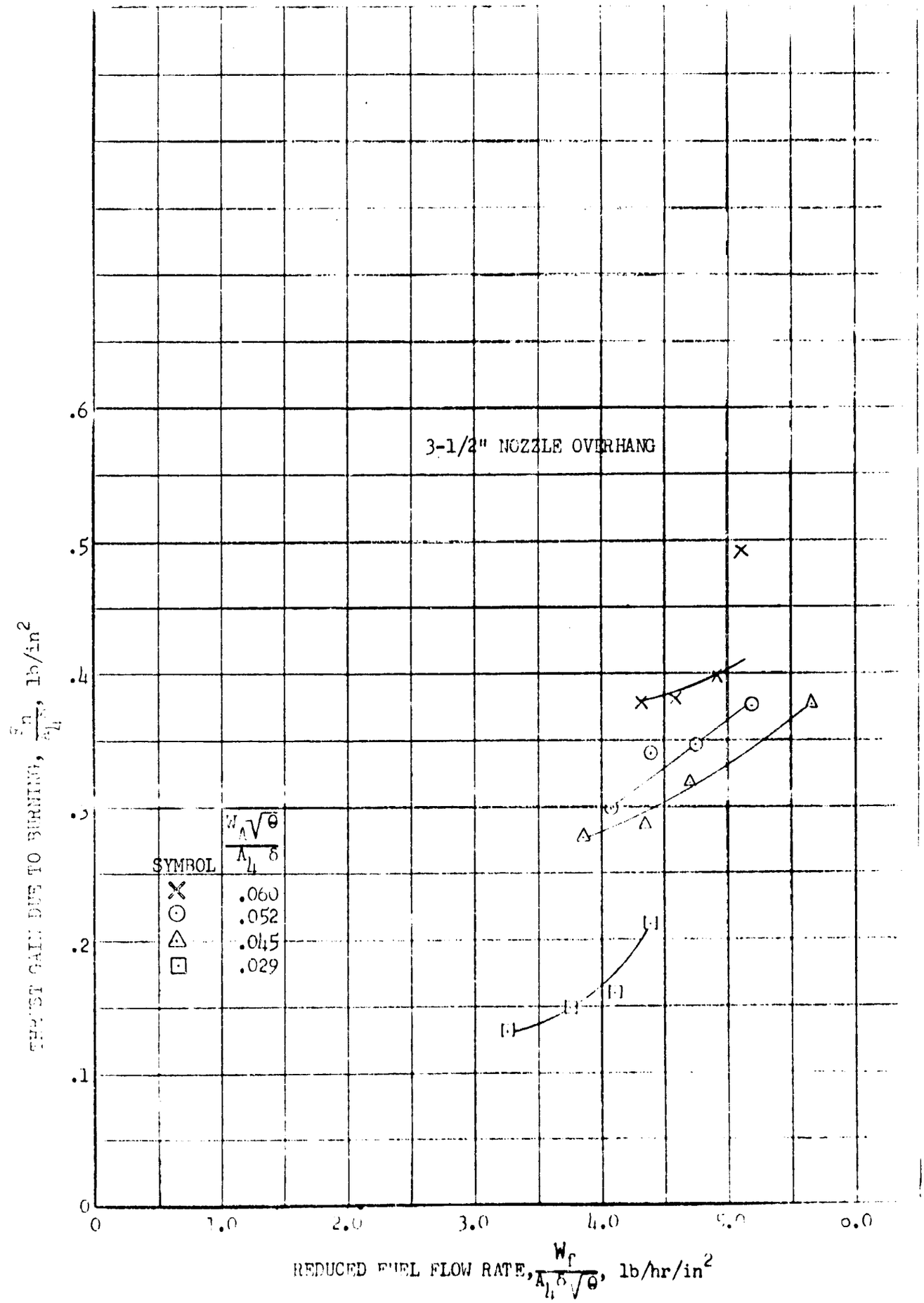
3-1/2" NOZZLE OVERHANG
SYMBOL
$\frac{W_A\sqrt{\theta}}{A_4\ \delta}$
.060
.052
.045
.029
0
.1
.2
.3
.4
.5
.6
1.0
2.0
3.0
4.0
5.0
6.0
THRUST GAIN DUE TO BURNING, $\frac{F_n}{A_4}$, lb/in^2
REDUCED FUEL FLOW RATE, $\frac{W_f}{A_4\ \delta\sqrt{\theta}}$, lb/hr/in^2

FIGURE 28

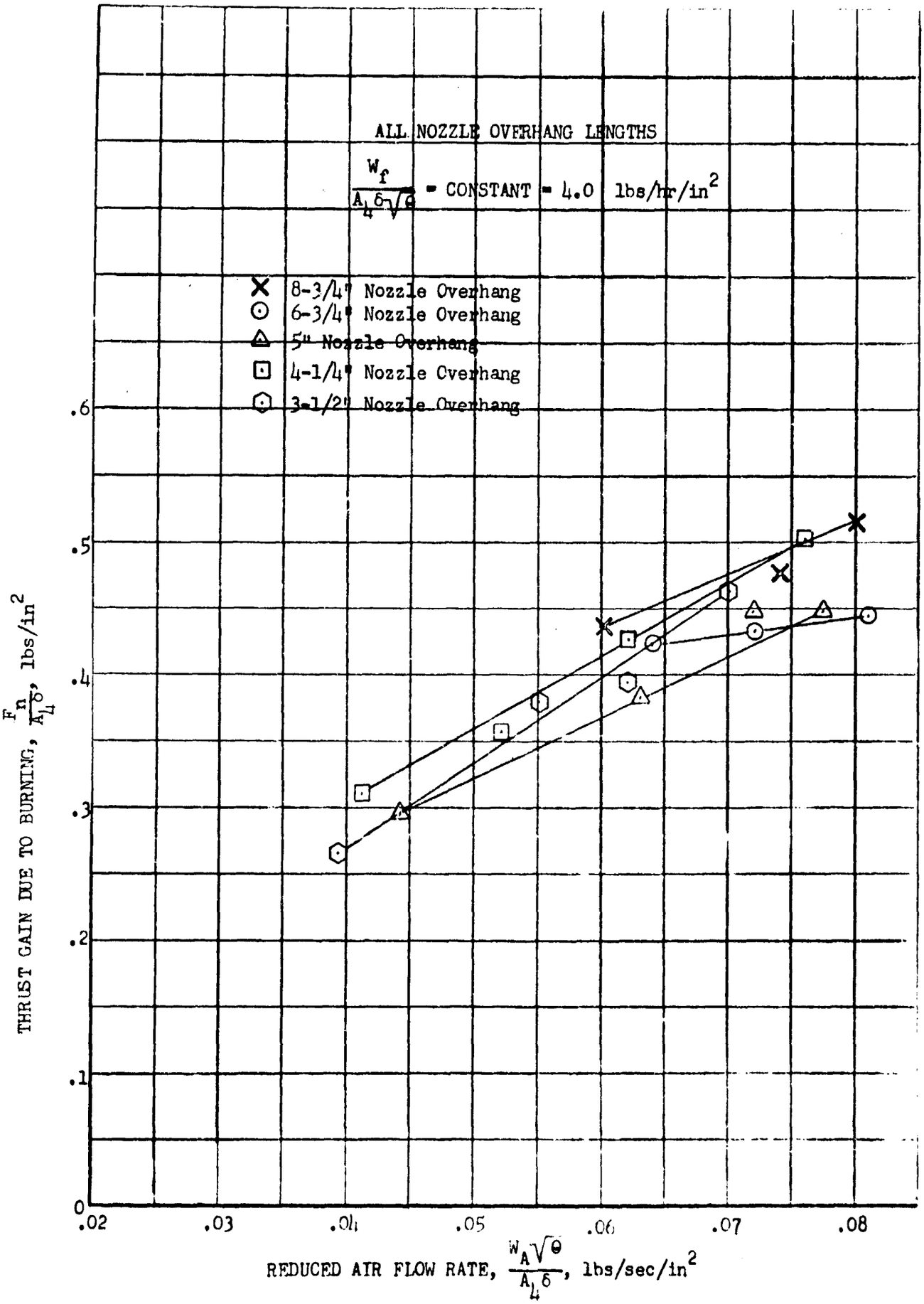
ALL NOZZLE OVERHANG LENGTHS
$\frac{W_f}{A_4 \delta \sqrt{\theta}}$ = CONSTANT = 4.0 lbs/hr/in^2
8-3/4" Nozzle Overhang
6-3/4" Nozzle Overhang
5" Nozzle Overhang
4-1/4" Nozzle Overhang
3-1/2" Nozzle Overhang
THRUST GAIN DUE TO BURNING, $\frac{F_n}{A_4 \delta}$, lbs/in^2
0
.1
.2
.3
.4
.5
.6
.02
.03
.04
.05
.06
.07
.08
REDUCED AIR FLOW RATE, $\frac{W_A \sqrt{\theta}}{A_4 \delta}$, lbs/sec/in^2

FIGURE 29

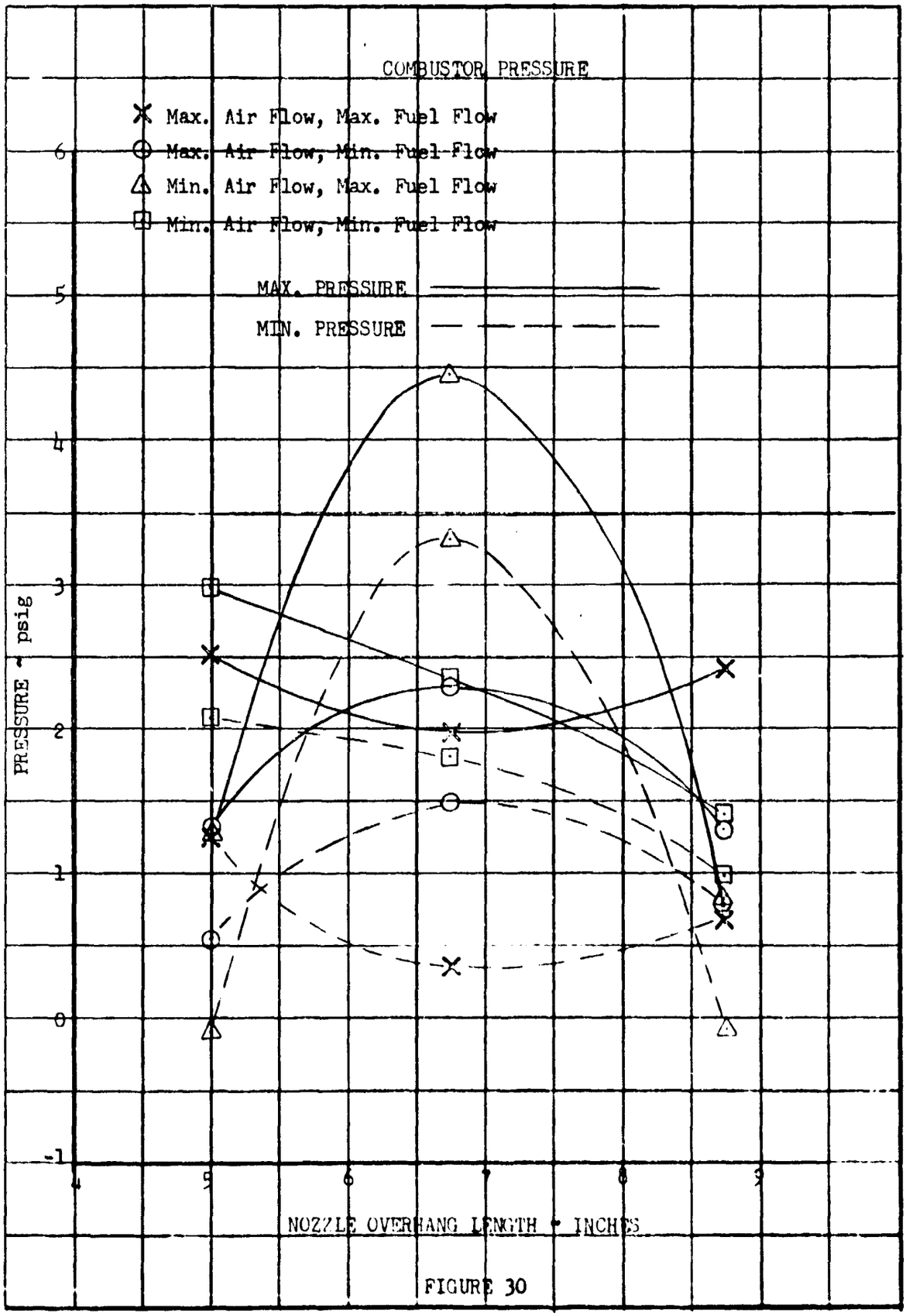
COMBUSTOR PRESSURE
Max. Air Flow, Max. Fuel Flow
Max. Air Flow, Min. Fuel Flow
Min. Air Flow, Max. Fuel Flow
Min. Air Flow, Min. Fuel Flow
MAX. PRESSURE
MIN. PRESSURE
PRESSURE - psig
6
5
4
3
2
1
0
-1
4
5
6
7
8
9
NOZZLE OVERHANG LENGTH - INCHES

FIGURE 30

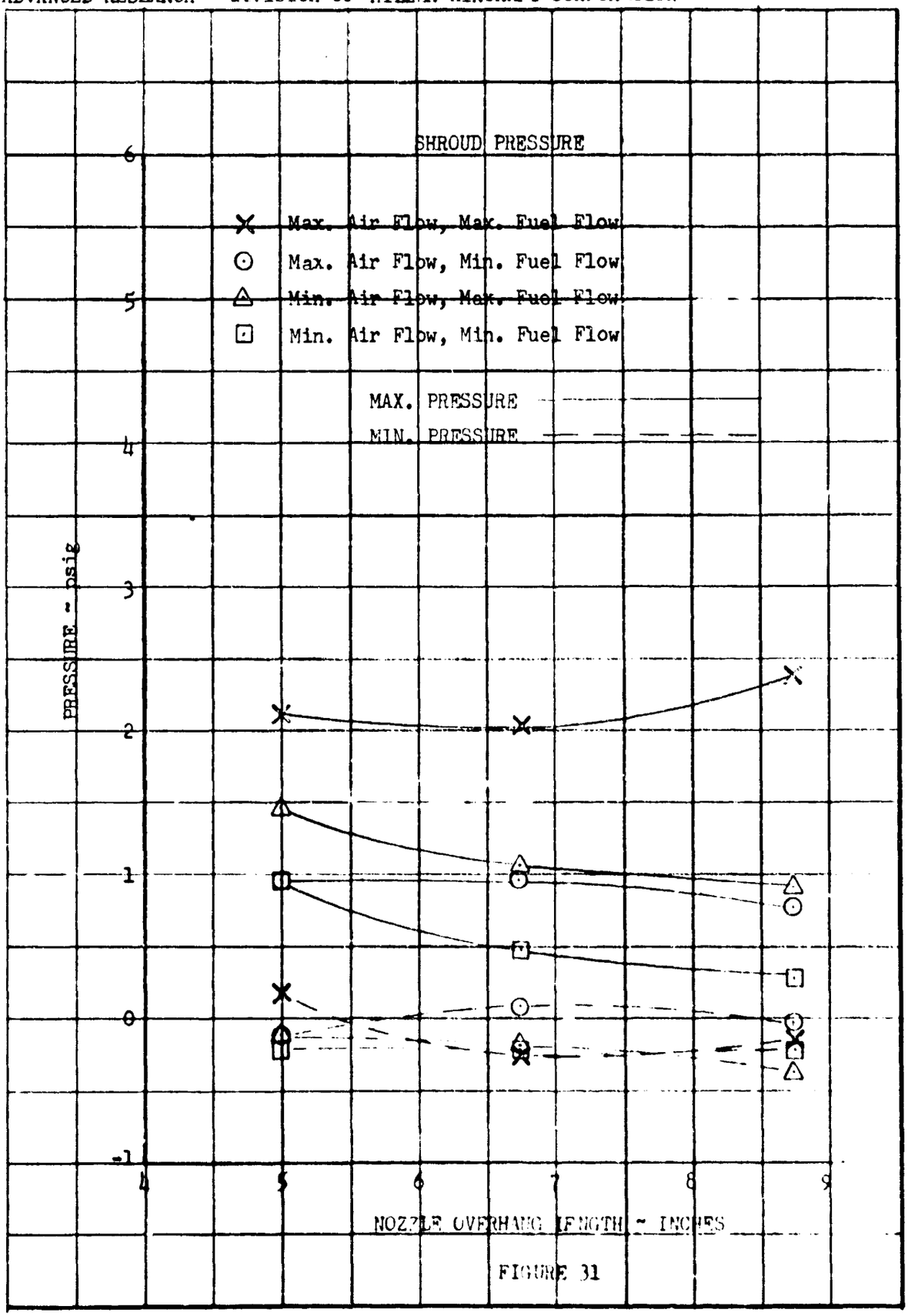
SHROUD PRESSURE
Max. Air Flow, Max. Fuel Flow
Max. Air Flow, Min. Fuel Flow
Min. Air Flow, Max. Fuel Flow
Min. Air Flow, Min. Fuel Flow
MAX. PRESSURE
MIN. PRESSURE
PRESSURE ~ psig
6
5
4
3
2
1
0
-1
4
5
6
7
8
9
NOZZLE OVERHANG LENGTH ~ INCHES

FIGURE 31

FIGURE 32: TABULATED VALUES FOR FIGURE (33)

(A)
W_A = 1.47 lbs/sec
W_F = 119.3 lbs/hr
F_R = 315 cps
F_n = 12.8 lbs
SFC = 9.33 lbs/hr-lb
$P_{t_4} - P_o$ = 1.26 "Hg
$\frac{P_{t_2} - P_{t_4}}{q_{A_{max}}}$ = 13.52

(B)
W_A = 1.76 lbs/sec
W_F = 41.5 lbs/hr
F_R = 290 cps
F_n = 4.6 lbs
SFC = 9.04 lbs/hr-lb
$P_{t_4} - P_o$ = .83 "Hg
$\frac{P_{t_2} - P_{t_4}}{q_{A_{max}}}$ = 8.68

(C)
W_A = .84 lbs/sec
W_F = 71.3 lbs/hr
F_R = 310 cps
F_n = 3.7 lbs
SFC = 19.26 lbs/hr-lb
$P_{t_4} - P_o$ = .38 "Hg
$\frac{P_{t_2} - P_{t_4}}{q_{A_{max}}}$ = 10.30

(D)
W_A = .89 lbs/sec
W_F = 34.5 lbs/hr
F_R = 290 cps
F_n = 1.7 lbs
SFC = 20.30 lbs/hr-lb
$P_{t_4} - P_o$ = .26 "Hg
$\frac{P_{t_2} - P_{t_4}}{q_{A_{max}}}$ = 9.47

(E)
W_A = 1.44 lbs/sec
W_F = 115.3 lbs/hr
F_R = 315 cps
F_n = 11.6 lbs
SFC = 9.95 lbs/hr-lb
$P_{t_4} - P_o$ = 1.15 "Hg
$\frac{P_{t_2} - P_{t_4}}{q_{A_{max}}}$ = 11.92

(F)
W_A = 1.58 lbs/sec
W_F = 59.5 lbs/hr
F_R = 290 cps
F_n = 6.2 lbs
SFC = 960 lbs/hr-lb
$P_{t_4} - P_o$ = .89 "Hg
$\frac{P_{t_2} - P_{t_4}}{q_{A_{max}}}$ = 10.08

(G)
W_A = .80 lbs/sec
W_F = 79.5 lbs/hr
F_R = 330 cps
F_n = 5.2 lbs
SFC = 15.28 lbs/hr-lb
$P_{t_4} - P_o$ = .45 "Hg
$\frac{P_{t_2} - P_{t_4}}{q_{A_{max}}}$ = 15.72

(H)
W_A = .89 lbs/sec
W_F = 36.0 lbs/hr
F_R = 290 cps
F_n = 2.2 lbs
SFC = 16.36 lbs/hr-lb
$P_{t_4} - P_o$ = .28 "Hg
$\frac{P_{t_2} - P_{t_4}}{q_{A_{max}}}$ = 8.91

(J)
W_A = 1.41 lbs/sec
W_F = 117.5 lbs/hr
F_R = 330 cps
F_n = 10.4 lbs
SFC = 11.30 lbs/hr-lb
$P_{t_4} - P_o$ = 1.15 "Hg
$\frac{P_{t_2} - P_{t_4}}{q_{A_{max}}}$ = 15.95

(K)
W_A = 1.58 lbs/sec
W_F = 59.4 lbs/hr
F_R = 295 cps
F_n = 5.8 lbs
SFC = 10.24 lbs/hr-lb
$P_{t_4} - P_o$ = .80 "Hg
$\frac{P_{t_2} - P_{t_4}}{q_{A_{max}}}$ = 12.44

(L)
W_A = .77 lbs/sec
W_F = 82.4 lbs/hr
F_R = 335 cps
F_n = 5.1 lbs
SFC = 16.16 lbs/hr-lb
$P_{t_4} - P_o$ = .42 "Hg
$\frac{P_{t_2} - P_{t_4}}{q_{A_{max}}}$ = 9.32

(M)
W_A = .80 lbs/sec
W_F = 54.5 lbs/hr
F_R = 315 cps
F_n = 2.9 lbs
SFC = 18.80 lbs/hr-lb
$P_{t_4} - P_o$ = .35 "Hg
$\frac{P_{t_2} - P_{t_4}}{q_{A_{max}}}$ = 10.32

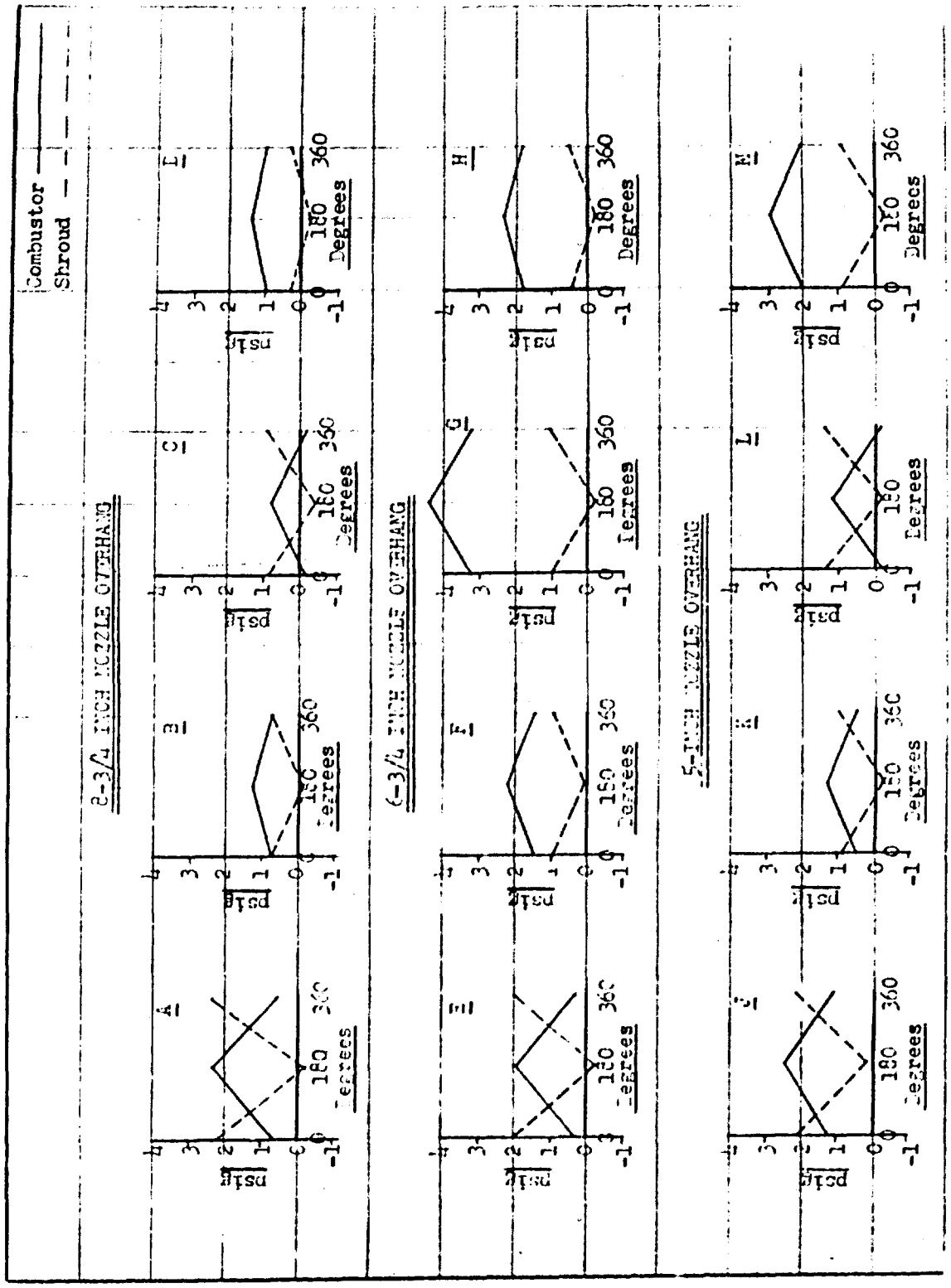

FIGURE 33: COMBUSTOR AND SHROUD PRESSURE CYCLES

								Actual	Theory	
	(1)	(2)	(3)	(4)	(5)	(6)	(7)	(8)	(9)	(10)
$\frac{W\sqrt{\theta}}{A\delta}$	Run No	Over Hang"	Air Speed	$\frac{F}{A\delta\theta}$	$\frac{P_{T4}-P_0}{\delta}$	$\frac{W_4\sqrt{\theta_0}}{A_{34}\delta}$	$\frac{T_{T4}}{\theta}$	$\frac{W_f}{A_{34}\sqrt{\theta_0}}$	$\frac{W_f}{\Delta_4 d\sqrt{\theta_0}}$	η_B
.060	28 H	6-3/4	175 ○	.732	.73	.061	1700	3.29	3.30	1.00
.060	29 H	↑	↑	.843	.86	.062	1925	4.48	3.35	.75
.066	30 H		↓	.464	.47	.066	875	.95	.96	1.01
.061	31 H		175	.589	.59	.062	1287	2.39	1.90	.79
.071	32 H		200	.982	1.00	.073	1625	5.34	3.80	.71
.077	33 H		↑	.636	.66	.077	1438	1.23	2.61	2.12
.071	34 H		↓	.747	.76	.072	1250	2.48	2.34	.94
.063	35 H		200	.894	.88	.064	1850	3.64	4.05	1.11
.050	36 H		150 △	.647	.65	.0512	2125	4.12	3.95	.96
.058	37 H		↑	.384	.38	.0586	925	.843	1.07	1.26
.056	38 H		↓	.456	.46	.0562	1225	2.11	1.84	.87
.052	39 H		150	.566	.58	.0529	1775	3.23	2.95	.91
.024	40 H		75 □	.197	.20	.0251	2335	2.30	2.30	1.00
.025	41 H		↑	.178	.18	.0308	560	1.92	1.41	.73
.025	42 H	6-3/4	75	.178	.1[illegible]	.0315	1560	2.12	1.41	.66
	46 H	5	150 △	.438	.44	.057	1150	1.777	1.80	1.01
	47 H	↑	↑	.487	.50	.056	1350	2.455	2.10	.86
	48 H		↓	.593	.60	.054	1725	3.98	3.10	.77
	49 H		150	.656	.67	.052	2075	4.86	4.05	.83
	50 H		175	.848	.87	.058	2261	5.22	3.90	.74
	51 H		↑	.598	.60	.065	1200	2.049	2.00	.97
	52 H		↓	.627	.63	.066	1250	2.770	2.18	.78
	53 H		175	.761	.78	.064	1638	4.062	3.30	.81
.032	59 H		100 ○	.333	.33	.0334	2375	3.732	3.15	.84
.035	60 H		↑	.289	.29	.0353	1925	2.716	1.91	.70
	61 H		↓	.314	.31	.0355	2025	2.836	2.61	.92
	62 H		100	.314	.31	.0351	2025	3.009	2.61	.84
.070	100 H		200 ▽	1.034	1.05	.071	1650	5.469	4.40	.80
.066	101 H		↑	.937	.96	.068	1775	3.487	3.95	1.13
	102 H	↓ ○	↓	.947	.97	.069	1776	4.193	3.98	.94
	103 H	5	200	1.010	1.03	.069	1850	4.781	4.41	.92

							Actual	Theory	
	①	②	③	④	⑤	⑥	⑦	⑧	⑨	⑩
$\frac{W\sqrt{\theta}}{A\delta}$	Run No	Over Hang "	Air Speed	$\frac{F}{A\delta}$	$\frac{P_{T4}-P_0}{\delta}$	$\frac{W_4\sqrt{\theta}}{A\delta}$	$\frac{T_{T4}}{\theta}$	$\frac{W_f}{A\delta\sqrt{\theta}}$	$\frac{W_f}{A\delta\sqrt{\theta}}$	η_B
	63 H	4-1/2	100 ⊙	.357	.36	.0302	3025	3.943	3.91	.99
	64 H			.314	.31	.0325	2275	3.058	2.82	.92
	65 H			.328	.32	.0325	2270	3.270	2.80	.85
	66 H		100	.353	.35	.0317	3000	3.819	3.90	1.02
	67 H		175 ⊙	.613	.62	.057	1650	3.270	3.00	.91
	68 H			.656	.67	.057	1725	3.842	3.32	.86
	69 H			.973	.79	.053	2350	5.147	4.75	.92
	70 H		175	.705	.72	.047	2750	4.342	5.10	1.16
	71 H		200 ▽	.947	.97	.061	2250	5.645	5.20	.92
	72 H			.894	.91	.071	1575	4.282	3.75	.88
	73 H			.918	.94	.069	1725	4.720	4.14	.87
	74 H		200	.923	.94	.070	1675	4.605	4.06	.88
	75 H		125	.578	.59	.041	2800	5.161	4.71	.91
	76 H			.438	.44	.045	1800	3.011	2.80	.92
	77 H			.496	.51	.045	2075	3.643	3.40	.93
	78 H	4-1/2	125	.573	.58	.042	2625	4.543	4.51	.99
.0603	79 H	3-1/2	200 ▽	.904	.92	.0619	2113	5.09	4.75	.93
.0599	80 H			.789	.81	.0612	1900	4.32	4.04	.93
	81 H			.803	.82	.0612	1915	4.59	3.50	.76
	82 H		200	.822	.84	.0603	2000	4.90	3.42	.69
	83 H		175 ⊙	.702	.72	.0523	2250	5.19	4.41	.84
	84 H			.630	.64	.0524	2000	4.08	3.75	.91
	85 H			.659	.67	.0583	1700	4.42	3.22	.72
	86 H		175	.673	.68	.0491	2375	4.73	4.51	.95
	87 H		150 △	.631	.64	.043	2825	5.642	5.07	.89
	88 H			.530	.54	.048	1975	3.909	3.42	.87
	89 H			.559	.57	.048	2050	4.348	3.62	.83
	90 H		150	.592	.60	.046	2250	4.712	4.00	.84
.031	91 H		100 ⊙	.361	.36	.032	2750	4.393	3.60	.82
.031	92 H			.270	.27	.031	2250	3.249	2.63	.80
	93 H			.289	.29	.028	2725	3.755	2.23	.59
	94 H	3-1/2	100	.303	.30	.029	2650	4.115	3.20	.78

$\frac{W\sqrt{\theta}}{A_4\delta}$	① Run No.	② Over Hang "	③ Air Speed	④ $\frac{F}{A_4\delta}$	⑤ $\frac{P_{T4}-P_0}{\delta}$	⑥ $\frac{W_4\sqrt{\theta}}{A_4\delta}$	⑦ $\frac{T_{T4}}{\theta}$	Actual ⑧ $\frac{w_f}{A_4\delta\sqrt{\theta}}$	Theory ⑨ $\frac{w_f}{A_4\delta\sqrt{\theta}}$	⑩ η_B
	95 H	3	100 ⊙	.304	.30	.027	2725	4.876	3.30	.67
	96 H	↑	100	.246	.25	.026	2475	3.305	2.75	.83
	97 H	↓	200 ▽	.771	.79	.055	2200	5.152	4.50	.87
	98 H	↓	100 ⊙	.258	.26	.026	2875	3.219	3.21	1.00
	99 H	3	100	.249	.25	.027	2750	2.902	3.00	1.03
.069	104 H	8-3/4	200 ▽	1.054	1.07	.071	1763	4.527	4.20	.93
.075	105 H	↑	↑	.713	.72	.075	1080	1.344	2.32	1.72
	106 H	↓	↓	.806	.82	.073	1350	2.519	2.81	1.11
	107 H	↓	200	.920	.94	.067	1825	3.591	2.00	.56
	108 H	↓	175 ⊙	.838	.86	.060	2050	3.792	3.55	.94
	109 H	↓	↑	.636	.65	.068	1175	1.357	2.00	1.40
	110 H	↓	↓	.708	.73	.066	1450	2.389	2.81	1.17
	111 H	↓	175	.770	.79	.067	1500	3.060	3.20	1.04
	112 H	↓	150 △	.470	.48	.063	1000	2.463	1.40	.57
	113 H	↓	↑	.616	.63	.050	2125	4.324	3.90	.90
	114 H	↓	↓	.494	.50	.052	1550	3.096	2.83	.91
	115 H	↓	150	.562	.58	.052	1825	3.741	3.20	.85
.031	116 H	↓	100 ⊙	.257	.26	.032	1975	2.797	2.21	.79
.032	117 H	↓	↑	.179	.18	.033	1375	2.132	1.20	.56
	118 H	8-3/4	100	.223	.22	.030	2000	2.562	2.14	.83